The Journal of Experimental Biology 206, 3405-3423

doi:10.1242/jeb.00583

Blubber and buoyancy: monitoring the body condition of free-ranging seals using simple dive characteristics

Martin Biuw[1,*], Bernie McConnell[1], Corey J. A. Bradshaw[2], Harry Burton[3] and Mike Fedak[1]

[1]*Sea Mammal Research Unit, Gatty Marine Laboratory, University of St Andrews, St Andrews, Fife, KY16 8LB, Scotland,* [2]*Antarctic Wildlife Research Unit, School of Zoology, University of Tasmania, GPO Box 252-05, Hobart, Tasmania 7001, Australia* and [3]*Australian Antarctic Division, Channel Highway, Kingston, Tasmania 7050, Australia*

*Author for correspondence (e-mail: emb7@st-and.ac.uk)

Accepted 2 July 2003

Summary

Elephant seals regularly perform dives during which they spend a large proportion of time drifting passively through the water column. The rate of vertical change in depth during these 'drift' dives is largely a result of the proportion of lipid tissue in the body, with fatter seals having higher (more positive or less negative) drift rates compared with leaner seals. We examined the temporal changes in drift rates of 24 newly weaned southern elephant seal (*Mirounga leonina*) pups during their first trip to sea to determine if this easily recorded dive characteristic can be used to continuously monitor changes in body composition of seals throughout their foraging trips. All seals demonstrated a similar trend over time: drift rates were initially positive but decreased steadily over the first 30–50 days after departure (Phase 1), corresponding to seals becoming gradually less buoyant. Over the following ~100 days (Phase 2), drift rates again increased gradually, while during the last ~20–45 days (Phase 3) drift rates either remained constant or decreased slightly. The daily rate of change in drift rate was negatively related to the daily rate of horizontal displacement (daily travel rate), and daily travel rates of more than ~80 km were almost exclusively associated with negative changes in drift rate. We developed a mechanistic model based on body compositions and morphometrics measured in the field, published values for the density of seawater and various body components, and values of drag coefficients for objects of different shapes. We used this model to examine the theoretical relationships between drift rate and body composition and carried out a sensitivity analysis to quantify errors and biases caused by varying model parameters. While variations in seawater density and uncertainties in estimated body surface area and volume are unlikely to result in errors in estimated lipid content of more than ±2.5%, variations in drag coefficient can lead to errors of ≥10%. Finally, we compared the lipid contents predicted by our model with the lipid contents measured using isotopically labelled water and found a strong positive correlation. The best-fitting model suggests that the drag coefficient of seals while drifting passively is between ~0.49 (roughly corresponding to a sphere-shaped object) and 0.69 (a prolate spheroid), and we were able to estimate relative lipid content to within approximately ±2% lipid. Our results suggest that this simple method can be used to estimate the changes in lipid content of free-ranging seals while at sea and may help improve our understanding of the foraging strategies of these important marine predators.

Key words: buoyancy, marine mammal, elephant seal, body composition, foraging ecology, satellite telemetry.

Introduction

With the development of time depth recorders (Kooyman, 1965) and satellite, radio and acoustic telemetry (e.g. Fancy et al., 1988; Fedak, 1992; Fedak et al., 1983; McConnell, 1986), it is now possible to study the behaviour of many free-ranging marine organisms. Although these data have provided new insights into the foraging ecology of marine species, there are still limitations in the types of information that can be collected. Specifically, direct observation or recording of feeding events is often impossible (particularly for animals ranging over large areas during extended trips), and it is consequently difficult to determine where and when individuals encounter and ingest food and how much of this is assimilated into the body energy stores. In some cases, instrumented individuals can be recaptured when they return to land, and their net growth, energy expenditure and change in body condition can be estimated and correlated with at-sea behaviour (Bost et al., 1997; Boyd et al., 1993; Boyd and Arnbom, 1991; Chappell et al., 1993; Kooyman et al., 1992; Le Boeuf et al., 2000). However, this only provides information on the relationship between body condition and the behaviour and movements integrated over months and thousands of kilometres, while we are frequently interested in

these relationships over scales of weeks and a few kilometres in order to more accurately correlate animal behaviour to fine-scale environmental features. To determine the timing and spatial pattern of food encounter at these finer scales, one must generally rely on indirect indices, such as movement patterns (e.g. Bell, 1991; McConnell, 1986), dive shape characteristics and/or measures of diving effort (Georges et al., 2000; Guinet et al., 2001; Lesage et al., 1999; Schreer and Testa, 1996). Although these methods have been useful for identifying potentially important foraging habitats, the degree to which these correspond to the rate of prey encounter and ingestion is still uncertain. Moreover, even if rates of prey encounter and ingestion could be inferred from these indices, they still do not provide information on the energy balance of the individual. For instance, an animal may have a high rate of prey encounter and capture but may still be in a negative energy balance if its activity and metabolic rates are high. Without information about these links, we cannot correctly estimate the food requirements and energy budgets of animals at sea.

Prey ingestion has been estimated by measuring changes in stomach or oesophageal temperature in seabirds (Garthe et al., 1999; Weimerskirch and Wilson, 1992; Wilson, 1992), sharks (Klimley et al., 2001), penguins (Charrassin et al., 2001; Putz and Bost, 1994; Putz et al., 1998), turtles (Tanaka et al., 1995) and seals (Bekkby and Bjorge, 1998; Gales and Renouf, 1993; Hedd et al., 1996). Although these techniques are useful for recording the timing of feeding events, estimates of meal size have generally been less reliable (Wilson et al., 1995), and the technique is further hampered by short retention times of stomach tags (Wilson et al., 1998). More recently, video and/or image recording instruments have been attached to seals and cetaceans in order to record the timing and rate of prey encounter (Davis et al., 1999; Hooker et al., 2002; Sato et al., 2002a), but the size of the resulting image data sets are often too large to be practical for deployments over more than a few days. Moreover, this technique only reveals what an animal encountered and not what it ingested, and because the body condition of an animal represents a balance between energy assimilation and expenditure, information about the timing of feeding and meal size is not sufficient for estimating the energy balance of an animal.

An alternative strategy is to use aspects of an animal's diving behaviour, as measured by existing data recorders, to indirectly estimate changes in body composition. One such approach is to monitor changes in the buoyancy of an animal through changes in measured dive characteristics (Beck et al., 2000; Crocker et al., 1997). In deep-diving phocids such as the elephant seal (*Mirounga* sp.), the buoyancy of an individual is determined primarily by its body composition and particularly by the ratio of lipid to lean tissue (Crocker et al., 1997; Webb et al., 1998). While lean tissue is denser than seawater, lipid tissue is less dense, and animals with a large proportion of lipid will therefore be more buoyant (Beck et al., 2000; Lovvorn and Jones, 1991a,b; Nowacek et al., 2001; Webb et al., 1998). Phocids that have seasonal cycles of terrestrial fasting and at-sea foraging demonstrate large fluctuations in body composition, and this should be reflected by changes in buoyancy (Beck et al., 2000; Crocker et al., 1997; Webb et al., 1998). Buoyancy can be estimated while an animal is drifting passively through the water column, and this behaviour is regularly observed in dive records from elephant seals (Crocker et al., 1997; Hindell et al., 1999; Le Boeuf et al., 1992). Drift dives were first defined by Crocker et al. (1997) and are broadly characterized by a rapid descent phase during which seals swim actively followed by a prolonged phase of slower descent or, less commonly, ascent during which seals are assumed to drift passively through the water column. The drift phase is typically followed by a period of active swimming and fairly rapid ascent to the surface. Although the function of drift dives is not clear, Crocker et al. (1997) suggested that they may play a role in food processing, predator avoidance and/or resting. We expect the rate of vertical descent or ascent during the drift phase to vary monotonically with the buoyancy of an animal, and this drift rate may therefore be used to track changes in an animal's body condition while at sea. Although this was demonstrated for female northern elephant seals (*Mirounga angustirostris*) by Crocker et al. (1997), they did not model these relationships to estimate the body condition of seals while foraging at sea using changes in drift rate.

Although the drift rate of a phocid seal will be determined largely by the proportions of lipid and lean tissue, it will also be affected by a variety of external and internal factors. By definition, the constant rate of vertical displacement (i.e. the terminal velocity) of an object moving through a medium occurs when all forces acting upon the object (i.e. gravity, buoyant force and drag resistance) are in equilibrium. The buoyant force is determined by the difference in density between the object and the surrounding medium, while the drag resistance is affected by the surface area and shape of the object, the density of the surrounding medium and the speed at which the object moves through this medium (Vogel, 1981). In terms of a seal drifting passively through water, the terminal velocity will be influenced by external characteristics, such as seawater density, that vary with salinity and temperature. It will also be influenced by physiological and behavioural changes such as residual air in the lungs and the orientation of the seal's body in the water. The interactions of all these variables will determine the accuracy with which the body composition of a seal can be estimated from observed drift rate.

In this study, we used ARGOS satellite telemetry (Argos, 1989) to relay dive and location data from recently weaned southern elephant seals (*Mirounga leonina*) from Macquarie Island during their first trips to sea. These data were used to describe the change in drift rate of individuals over time. To assess the accuracy of estimating buoyancy and body composition of individual seals from observed drift rates, we developed a theoretical mechanistic model of a typical seal pup and examined the relative contributions of various potential error sources. Finally, we assessed the accuracy of our model by comparing the body composition of a seal predicted from drift rates just after departure from Macquarie Island with the

body composition measured just before departure. Throughout this paper, we have adopted the operational definition of body composition as referring to percent body lipid.

Materials and methods

Study animals and capture

We selected our study animals from a larger sample of individually marked, recently weaned southern elephant seal pups (*Mirounga leonina* Linnaeus 1758) from the northern isthmus breeding colony at Macquarie Island (54°30′ S, 158°57′ E). These pups had previously been weighed and measured at birth and weaning as part of a large-scale mark/recapture program (McMahon et al., 2000b). The study was performed in two stages. In the first stage, we deployed 44 instruments (32 in 1995 and another 12 in 1996) to study the ontogeny of migration and diving behaviour in naïve pups (Hindell et al., 1999; McConnell et al., 2002). In the second stage, we deployed another 23 instruments on female pups (15 in 1999 and eight in 2000) as part of a detailed investigation of changes in body composition and survival of pups after weaning.

Seals were captured and weighed according to McMahon et al. (2000a). The axial girth (*AG*) was measured immediately caudal to the base of the pectoral flippers, and the length was measured as the straight line between the tip of the nose and the tip of the tail (referred to as standard length, or L_{st}). Seals were then lightly sedated with an intravenous dose of tiletamine/zolasepam [Zoletil® 100 (Virbac, Peakhurst, NSW, Australia) or Telazol® (Wildlife Pharmaceuticals Inc., Fort Collins, CO, USA)] at an approximate dose rate of 0.2–0.4 mg kg^{-1} (Field et al., 2002). Satellite Relayed Data Loggers (SRDLs; Sea Mammal Research Unit, St Andrews, UK) were glued to the fur on the head or upper neck region using two-component industrial epoxy glue (Hilti; Silverwater, NSW, Australia) according to the methods described in Fedak et al. (1983), Hindell et al. (1999) and McConnell et al. (2002). We monitored the breeding beaches on a daily basis, and if seals were still present at the colony more than one week after deployment they were captured again and re-weighed.

Body composition

In 1999 and 2000, we used isotopically labelled water (e.g. Nagy and Costa, 1980; Reilly and Fedak, 1990) to measure the body composition of pups at weaning, prior to departure and upon return to the island. Immediately after sedation, a blood sample was collected from the extradural vein to measure the background isotope level. A weighed dose of approximately 7.4×10^4 Bq tritiated water (^{3}HHO) in 4 ml of distilled water was then injected using a 5 ml plastic syringe. The syringe was flushed with blood three times to ensure complete delivery of the ^{3}HHO. A second blood sample was taken 2–3 h after initial injection for determination of dilution space and calculation of body composition. Blood samples were centrifuged and the plasma transferred to 2 ml cryotubes, which were stored at –20°C until further analysis.

We analysed plasma samples for ^{3}H specific activity by liquid scintillation counting. Weighed plasma samples of approximately 100 μl were added to 10 ml of PicoFlour scintillation cocktail (Packard Instruments) and counted in triplicate for 10 min on a Packard Tri-Carb® 2000 liquid scintillation counter. Correction for quenching was made by automatic external standardization. We prepared standard dilutions by gravimetric dilution of an aliquot part of the injectate to the approximate dilution expected in the seals, and these were also counted in triplicate for 10 min. The exact water content of each plasma sample was determined by transferring ~100 μl of the sample to a weighed glass slide. The slide was weighed again and then dried on a hot plate at a temperature of ~50°C until complete evaporation of the plasma water had been achieved, after which the slide was weighed a third time. In this way, we could correct the specific activity of ^{3}H for the exact plasma water content.

We calculated total body water (*TBW*), according to the empirically derived equation for grey seals (*Halichoerus grypus*; Reilly and Fedak, 1990), as:

$$TBW = -0.234 + 0.971(^3\text{HHOspace}) . \quad (1)$$

The total amount of lipid (*TBL*) and protein (*TBP*), expressed as percent of body mass (M_b), total body ash (*TBA*) and total body gross energy (*TBGE*; expressed in MJ) were also calculated according to Reilly and Fedak (1990):

$$\%TBL = 105.1 - 1.47(\%TBW) , \quad (2)$$

$$\%TBP = 0.42(\%TBW) - 4.75 , \quad (3)$$

$$TBA = 0.1 - 0.008(M_b) + 0.05(TBW) , \quad (4)$$

$$TBGE = 40.8(M_b) - 48.5(TBW) - 0.4 . \quad (5)$$

On-board data interpretation and compression

SRDLs collect and store dive parameters using various sensors and later relay dive records in compressed form *via* the ARGOS system. Depth was measured by the pressure transducer and circuitry on board the SRDL (Keller PA-7; Keller, Winterhur, Switzerland). The output from the depth transducer was sampled with 16-bit A/D such that, after calibration and offset correction, it provided an accuracy of 0.20 m. Swim speed was recorded by a turbine odometer (Logtron; Flasch Electronik GmbH, Munich, Germany; stall speed ≤0.25 m s^{-1}) housed in a polyurethane dome on top of the SRDL housing. Because the SRDL was mounted on the dorsal surface of the head, it would only be expected to respond to movement through the water if the seal was swimming nose first. The SRDLs recorded data every four seconds throughout a dive, and at the end of each dive these data were processed and compressed by the on-board microprocessor and stored in the short-term memory before being relayed *via* the ARGOS satellite system. The details of the compression algorithm are described in Fedak et al. (2001), and the general telemetry system is presented in Fedak et al. (2002). The dive data stored

and transmitted back from the instrument make up two categories: (1) 'summary dives', for which only maximum dive depth and duration are stored and transmitted, and (2) 'detailed dives', for which all inflection points and speed data are calculated and transmitted. The transmitted parameters describing a detailed dive are (1) total dive time, (2) the four most important inflection points (d_1–d_4; Fig. 1) with the most rapid change in dive trajectory, and (3) three mean swim speeds (U_1–U_3; Fig. 1). The first mean swim speed (U_1) is calculated from all recorded swim speeds between the start of the dive and the first inflection point (d_1), U_2 is calculated between d_1 and d_4, and U_3 between d_4 and the end of the dive (Fig. 1).

Selection of drift dives

We used a combination of methods for selecting drift dives for analysis and, because of differences in the software controlling the SRDLs' data collection and compression used in different years, the combination of selection criteria varied between instruments.

The first method for the selection of drift dives was that U_2 is equal to zero (i.e. less than the stall speed), while U_1 and/or U_3 are less than 0. There are two problems with this method: (1) the speed sensor can sometimes get blocked by debris, resulting in erroneous recordings of swim speeds of 0, and (2) the putative drift phase of a dive does not always correspond to the total time between d_1 and d_4 for which U_2 is measured (see also the description for the second method below), and actual drift dives may therefore occasionally have a U_2 not equal to 0. We therefore used a second method based on the dive profile rather than swim speed. The shape of the putative drift segment was examined by fitting different regression lines through; (1) all inflection points or excluding (2) the first or (3) the last inflection point. We used the line of best fit by selecting the model with the lowest mean squared residual (MSR), and the corresponding interval was selected as the putative drift phase. The drift rate (in cm s^{-1}) was defined by the slope coefficient for the regression line of the selected segment. The MSR of the best-fitting line also provided an 'index of linearity' of the selected phase. After initial visual examination of 1000 dive shapes and their corresponding MSR values, we subsequently rejected all dives with an MSR of >5 m^2.

The final method was based on maximum dive depth and the duration of the putative drift phase. We only selected dives where the depth of the shallowest inflection point was at least 10 m and where the drift phase represented more than 40% of the total duration. Although these criteria may have excluded some shallow drift dives of short duration, the drift phase for these dives would be too short to allow a meaningful estimate of drift rate to be calculated. It also minimized the risk of including dives for which air left in the airways may have a significant effect on the buoyancy of an animal (see detailed discussion below).

Overview of numerical and statistical analyses

Once drift dives had been selected, we went through a series of analyses to test their usefulness for predicting body condition. First, we used a smoothing algorithm to fit a function to the drift rate records for each individual seal, allowing us to define a representative daily value of drift rate. Second, daily changes in drift rate were calculated from these fitted values. The predictive functions were then inspected to define phases of the trip with contrasting characteristics, and these definitions were compared with one commonly used criterion for defining putative travelling and foraging phases: daily travel rate. Third, we constructed a mechanistic model of drift dives in relation to body composition, morphometrics (i.e. surface area and volume), residual lung volume, drag coefficient (C_D) and seawater density. We tested the sensitivity of this model to variations in the parameter values for these variables using bootstrap resampling. Finally, we tested the model by comparing the predicted body composition immediately after departure with the body

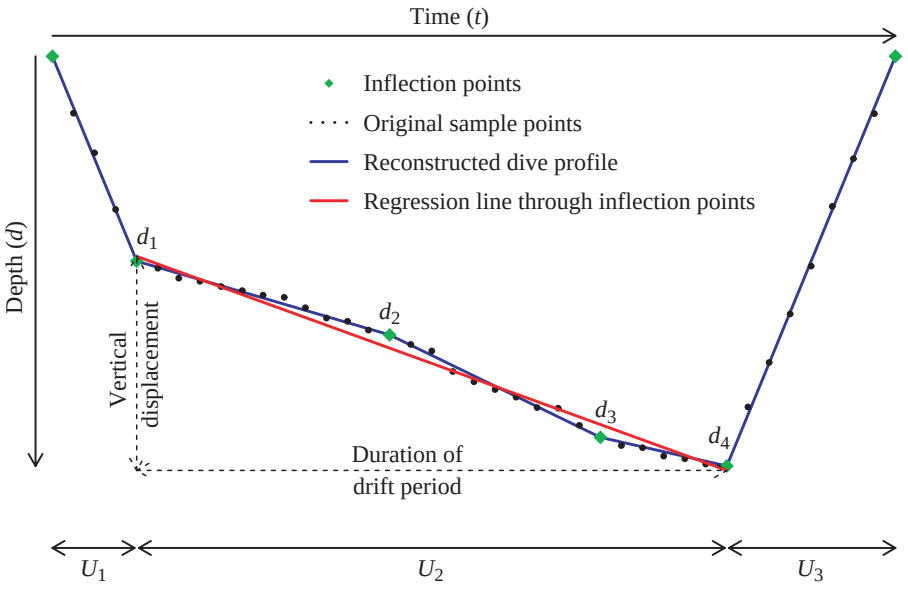

Fig. 1. Schematic representation of a drift dive, showing the original sampling points, the inflection points stored and transmitted by the Satellite Relay Data Logger (SRDL) and the reconstructed time–depth profile. The drift rate is calculated as the slope coefficient ($\Delta d/\Delta t$) of the best-fitting regression line. Here, only the regression line for the entire segment between d_1 and d_4 is shown, but in the actual selection process three different regression lines were evaluated (see text for further details).

composition measured using labelled water immediately before departure.

Time series and fitted daily values

We used a non-parametric smooth spline technique [smooth.spline (Venables and Ripley, 1994), as implemented in the R package (Ihaka and Gentleman, 1996)] to fit a predictive function to the time series of drift rates for each individual seal. The fitted values from these curves were taken to represent the expected drift rate for an individual seal on a given day. Spline functions divide the range of observed values by an ordered set of points (knots) along the x (time)-axis. Within each interval, the fitted curve is a cubic polynomial, and over the whole range the fit is further constrained to have continuous first and second derivatives at the knot locations. The curve is normally fitted by generalised cross-validation (GCV) (Gu and Wahba, 1991; Venables and Ripley, 1994), resulting in a curve that represents the best compromise between goodness-of-fit and degree of smoothness. We constrained the algorithm further by setting the initial intervals between knots to 14 days. The final interval length was then fine-tuned by the GCV algorithm. We chose 14 days as our interval to reduce the risk of over-fitting due to occasional high sensitivity to local minima, while also allowing for biologically realistic changes in drift rate expected to be detectable over a period of 5–6 days (see Methods and Results).

Prior to fitting the spline curve, we square transformed the drift rate values. This was done because the quadratic relationship between drag and velocity (see equation 8) results in a time record of change in drift rate with marked discontinuities around zero drift rate (i.e. neutral buoyancy). Transforming the drift rates prior to fitting allowed us to obtain a more continuous distribution, thereby aiding the spline-fitting algorithm. The squared drift rate values, along with the fitted daily values, were then back-transformed for further analyses.

Correlation with travel rate

It is common in analyses of animal movements to divide trips into different periods of putative travelling and foraging, and one way to do this is by defining some threshold value for daily horizontal displacement (see e.g. Hindell et al., 1999; McConnell et al., 2002). In order to examine how daily horizontal displacement (hereafter referred to as 'travel rate') corresponds to drift rate, we also defined three phases based on daily changes in observed drift rate. Following Hindell et al. (1999) and McConnell et al. (2002), we determined the transitions between Phases 1 and 2 and between Phases 2 and 3, respectively, as the first and last days where the five-day running average of daily travel rate was less than 20 km. This horizontal displacement is the net displacement over a 24-h period and may or may not correspond to the total distance travelled over the same period, depending on the directionality of the movements taken by the animal. In terms of drift rates, we defined these transitions as the first and last days when an individual seal showed a positive daily change in the smoothed drift rate. In order to define the maximum change in drift rate likely to be observed for a given daily travel rate, we performed quantile regressions (Koenker and Bassett, 1978) as implemented by the rq function in the R package quantreg. This function fits conditional regressions through a specified quantile (in this case, the 90th quantile) of a response variable.

Drift rate and body composition

To test the accuracy of body composition estimated from drift rates, we developed a theoretical mechanistic model of drift rate for a hypothetical average elephant seal pup at Macquarie Island. Typical values for standard nose-to-tail length (L_{st}) and axial girth (AG) were taken from all pups captured as part of the larger study in 1998, 1999 and 2000 investigating body composition of pups. For simplicity, we kept the volume of the pup constant at 100 litres and varied the lipid content between 10% and 60%. The proportions of other body components were then derived from equations 2–5 above. The total density of the seal over the range of body compositions was calculated according to:

$$\rho_{seal} = (\rho_l \times P_l) + (\rho_p \times P_p) + (\rho_b \times P_b) + (\rho_{bw} \times P_{bw}) , \quad (6)$$

where ρ is the density of the component, P is the proportion of the component, and subscripts l, p, b and bw indicate lipid, protein, bone mineral (ash) and body water, respectively (e.g. P_l=0.01×%TBL from equation 2 above). We used published values for the density of various body components in humans (Moore et al., 1963). These values were ρ_l=0.9007 g cm^{-3}, ρ_p=1.340 g cm^{-3}, ρ_b=2.300 g cm^{-3} and ρ_{bw}=0.994 g cm^{-3}. We then modelled the buoyant force according to Vogel (1981) as the difference between the total density of the body and the surrounding seawater:

$$BF = (\rho_{sw} \times \rho_{seal}) \times V \times \boldsymbol{g} , \quad (7)$$

where BF is the buoyant force in N, ρ_{seal} is the density of the seal in g cm^{-3}, ρ_{sw} is the density of the surrounding seawater, V is the volume of the seal in cm^3, and $\boldsymbol{g}$ is the gravity constant. The drag force (D) of the seal was estimated by:

$$D = \tfrac{1}{2} \times C_D \rho_{sw} S \mathbf{V}^2 , \quad (8)$$

where C_D is the dimensionless drag coefficient, S is the surface area of the seal in m^3, and $\mathbf{V}$ is the terminal velocity in m s^{-1} (Vogel, 1981). The theoretical drift rate could then be calculated as the terminal velocity by equating the previous two equations:

$$\mathbf{V} = \sqrt{2 \times \frac{(\rho_{sw} - \rho_{seal}) V \boldsymbol{g}}{C_D \rho_{sw} S}} . \quad (9)$$

Using this equation, we could then quantify the relative importance of variations in seawater salinity and temperature, seal surface area and C_D on the predicted drift rate. The maximum and minimum seawater densities were calculated based on the maximum salinity, temperature and depth ranges likely to be encountered by elephant seals from Macquarie Island. The temperature and salinity ranges were taken from Gordon (1988) and were 0–6°C and 33.9–34.7‰, respectively.

The depth range over which seawater densities were calculated was set to 0–500 m. The surface area of the seal was initially modelled as two opposing cones with a common base, the circumference of which corresponded to the *AG* of a typical seal pup (135 cm). The anterior cone was assumed to have a height corresponding to one-third of the mean standard L_{st} of a typical seal pup (135 cm), while the posterior cone had a height of two-thirds of the mean L_{st}. Williams and Kooyman (1985) reported a C_D of 0.09 for a harbour seal (*Phoca vitulina*). However, this was for an actively swimming animal, travelling headfirst and thereby minimising drag. It is unlikely that a passively drifting seal will move in the same streamlined orientation, and we therefore tested a range of coefficients. Here, we assumed a Reynolds number of a seal in ~10°C water to be ~60 000 at a speed of 0.25 m s^{-1} and ~120 000 at a speed of 0.5 m s^{-1}. This gives C_D values of ~0.47 for a sphere and 1.17 for a cylinder travelling crosswise. In our initial analyses, we therefore used these three values (0.09 for the harbour seal, 0.47 for a sphere and 1.17 for a cylinder). These values were slightly modified in subsequent analyses (see below).

The total buoyancy of an air-breathing aquatic animal is not constant but will change with depth due to residual air in the lungs, which is compressed at greater depths. We used published equations for the relationship between body size and residual lung volume to estimate the likely bias caused by this residual air. Kooyman (1989) estimated the residual lung volume of a marine mammal at the onset of a dive to be about 50% of the total lung capacity (*TLC*), where *TLC* (in litres) is estimated as:

$$TLC = 0.10(M_b)^{0.96} . \quad (10)$$

While this equation assumes that *TLC* is approximately proportional to the total body mass, we instead assumed *TLC* to be proportional to the lean body mass of the seal. However, while equation 10 estimates the lungs to be roughly 10% of total body mass (i.e. a constant of 0.10), we compensated for the use of lean mass instead of total mass for our calculations and assumed that the lungs represent ~12.5% of total lean mass (i.e. using a constant of 0.125). This correction was based on the assumption that the mean lean mass of the seals studied by Kooyman (1989) was ~70% of total body mass and that a lung volume of ~10% of total body mass is roughly equivalent to a lung volume of ~12.5% of lean mass. To simplify our calculations, we also substituted lean mass with lean *volume*, since our model seal had a total body volume set to 100 litres. This gave us the following relationship between seal lean volume (V_l), depth (d) and air volume at a given depth ($V_{a,d}$):

$$V_{a,d} = \frac{0.0625 \times V_l^{0.96}}{1 + (d/10)} . \quad (11)$$

The estimated density for a seal with a given body composition at a given depth ($\rho_{seal_{a,d}}$) could then be calculated as:

$$\rho_{seal_{a,d}} = \frac{\rho_{seal} \times V_t}{V_t + V_{a,d}} , \quad (12)$$

where V_t is the total body volume. This adjusted density could then be used in equation 9 to calculate the estimated drift rate for the specific depth according to:

$$\mathbf{V} = \sqrt{2 \times \frac{\left(\rho_{sw} - \frac{\rho_{seal} \times V_t}{V_t + V_{a,d}}\right) V\boldsymbol{g}}{C_D \rho_{sw} S}} . \quad (13)$$

Because seals change depth during drift dives, the residual lung volume will also change, as will the total body density. To simplify our model, we have defined depth as the midpoint between the start and end depth of the drift phase, and thus the predicted drift rate would correspond to the rate halfway through the drift phase.

Model evaluation

1. Simulation test

We tested the sensitivity of the model to the various parameters using a randomised bootstrap procedure. One hundred drift dives were randomly selected from the total sample of observed dives. These dives were selected with replacement (i.e. a dive could be selected more than once), and the drift rate and the depth halfway between the start and end depths of the drift segment (mid-depth) for each of these dives were extracted. For each dive, values of *AG*, L_{st}, C_D and ρ_{sw} were drawn at random from populations of 1000 values, following realistic distributions for these variables; *AG* and L_{st} were drawn from normal distributions with means ± S.D. of 1.3±0.1 m and 1.5±0.1 m, respectively (based on all measurements on pups in the larger body composition study before and after the first trip). Drag coefficients were drawn from a uniform distribution with minimum and maximum values of 0.47 (sphere) and 1.17 (cylinder), and seawater densities were drawn from a uniform distribution with minimum and maximum values of 1.027 g cm^{-3} and 1.030 g cm^{-3}, respectively. The body surface area and volume were calculated from the *AG* and L_{st} values as previously described, and the volume of residual air in the lungs was calculated based on this body volume for the specific mid-depth value for each of the 100 selected dives.

We then calculated the predicted body density by re-arranging equation 13:

$$\rho_{seal} = \frac{\left(\rho_{sw} - \frac{\mathbf{V}^2(C_D \rho_{sw} S)}{2V_t \boldsymbol{g}}\right)(V_t + V_{a,d})}{V_t} , \quad (14)$$

and a lipid content was then derived from this density using equation 6. This lipid content is hereafter referred to as 'predicted' lipid content.

We compared this set of 100 predicted lipid contents to a set of 'actual' lipid contents that were calculated assuming an L_{st} and *AG* of 1.5 m and 1.3 m, respectively, a seawater density of 1.028 g cm^{-3} and a C_D of 0.82, i.e. the average of the C_D values for a sphere (0.47) and a cylinder (1.17). We calculated the kernel density distribution of all 100 residuals (predicted to

actual lipid contents) and defined the range of errors corresponding to a probability density of >0.025 to obtain 95% confidence intervals for our prediction accuracies. We repeated the whole procedure 1000 times and thus obtained mean and variance estimates for the confidence intervals of the prediction errors. We first ran this procedure allowing values for all parameters to be randomly selected and then repeated the procedure keeping all but one of the parameters fixed. This allowed us to estimate how uncertainty in each parameter estimate contributed to the overall error. We also ran two separate series of analyses, one using uncorrected body density values and the other using values corrected for the assumed volume of residual air at the mid-depth of the drift segment. This allowed us to estimate both the likely bias due to residual air in a real data set and also to determine if the error range was similar for uncorrected and corrected values. In the first case, uncorrected predicted values obtained from the simulation procedure were compared with uncorrected actual values obtained by keeping all parameters fixed (as described above), while in the second case both the predicted and actual values were first corrected for the residual air volume at the mid-depth.

2. Correlation between predicted and measured lipid content

The final test of our model was to compare the lipid contents predicted from drift rates with lipid contents measured using labelled water immediately prior to departure (hereafter referred to as 'measured' lipid contents), as described above. Because many SRDL records ended well before animals returned to land, we did not include comparisons of predicted and measured lipid contents when seals returned after an extended foraging trip.

In this analysis, the volume (V) and surface area (S) of each individual was calculated from the AG and L_{st} measurements made just prior to departure, assuming the seal was shaped like a prolate spheroid. The functions for calculating volume and surface area were thus:

$$V = \tfrac{4}{3}\pi r_{AG}^2 r_{L,st} \quad (15)$$

and

$$S = 2\pi r_{AG}^2 + 2\pi \frac{r_{AG} r_{L,st}}{e} \sin^{-1} e\,, \quad (16)$$

where r_{AG} is the axial radius calculated from the axial girth, $r_{L,st}$ is the longitudinal radius calculated as $0.5\times L_{st}$, and e is calculated as:

$$e = \sqrt{1 - \frac{r_{AG}^2}{r_{L,st}^2}}\,. \quad (17)$$

For each dive, we then calculated the residual lung volume as a function of seal volume as described above, using the depth halfway between the start and end depth of the drift segment. Finally, we were then able to determine a predicted lipid content for each dive corresponding to the drift rate of that dive. This gave us an individual time series of predicted lipid contents for each individual over the duration of the SRDL record, and representative daily values were again calculated by fitting spline functions (knot intervals = 14 days) to these time series according to the methods described above. The predicted lipid content for each seal at the day of departure was then compared with the lipid content measured for that seal using labelled water. Since the labelled water method gives values for lipid content in mass percent, all lipid contents predicted from drift rates were multiplied by the previously published value of 0.9007 for lipid density (Moore et al., 1963) to convert them from percent by volume to percent by mass.

In this analysis, we included C_D as a parameter to be estimated by the model and tested the fit across the entire range of C_D values, from the harbour seal (0.09) to the cylinder (1.17). We used two different methods for assessing the fit. The first method selected the C_D that gave the smallest sum of squared residuals between predicted and measured lipid contents. The second method was based on the slope of the regression line between predicted and measured lipid contents and selected a C_D that gave a slope coefficient of 1. The rationale of using these two methods was that the C_D value giving the smallest absolute errors between predicted and measured lipid contents may have a slope that is significantly different from 1, i.e. that the errors are dependent on the absolute values of lipid content. For instance, a slope of >1 would suggest that for fatter animals the model produces values of lipid content that are underestimated compared with measured lipid contents, while it gives overestimated lipid contents for leaner seals, and *vice versa* if the slope coefficient is <1.

Temporal resolution of fitted time series

Our model also allowed us to obtain a rough estimate of the period over which we can detect a true trend in drift rate given the amount of random noise in the data. The daily lipid gain is likely to be relatively small in proportion to the lipid already present in the body. This will affect the time scale over which we can detect a significant change in drift rate. We also expect some variations in drift rate observed within a given day due to changes in body orientation within and between dives and variations in residual lung volume. To estimate the likely effects of these variations, and to determine the likely temporal resolution of our method, we compared the estimated daily change in drift rate for a feeding seal with the mean daily residuals of drift rate (i.e. the difference between each observed drift rate for a given day and the mean drift rate for that day obtained from the fitted spline function). We modified our mechanistic model to estimate the mean observed change in drift rate over the foraging period and to estimate the likely daily change. We again assumed a total body volume of 100 litres at departure, of which 38% is lipid, and 150 litres at return 175 days later, of which 32% is lipid (Sea Mammal Research Unit, unpublished data). We estimated a mean foraging period of 100 days, starting 30 days after departure. We also estimated the volume and body composition at the start of feeding based on the values at departure, assuming that the metabolic rate of a seal while in transit is similar to that on land. Similarly, we estimated the volume and body

composition at the end of feeding by back-calculating from values at return to the island 45 days later, again assuming a metabolic rate while in transit similar to that on land. From these values, we estimated a mean daily change in lipid content and calculated the expected mean daily change in drift rate. We could then compare this daily change to the daily residuals. These calculations were done for each seal separately, and the probability distributions of the residuals were modelled as kernel density functions. We selected the residual value corresponding to the maximum kernel density value as our best estimate of within-day variation in drift rate for a given seal. By dividing this value by the estimated mean daily change in drift rate we could then determine the minimum time interval over which any changes in drift rate would be likely to represent a real change in body composition.

All descriptive statistics are presented as means ± 1 S.D., unless stated otherwise.

Results

Drift dive extraction and summary

We obtained drift dive records that were of sufficient duration and continuity to allow for proper statistical analysis from 24 individual seals (Table 1). Of these seals, four belonged to the 1996 cohort (three males and one female), 12 from the 1999 cohort (all females) and eight from the 2000 cohort (all females). In total, 74 999 dives with complete profiles were recorded. Of these, 2746 dives fitted our selection criteria for drift dives, and the number of dives extracted for each seal varied from 26 to 210. The mean number of drift dives obtained per day for an individual seal varied from 1.23 to 3.74 (2.29±0.58), and the maximum number of dives obtained ranged from 3 to 14 dives per seal daily. Most of the dives extracted (2144 dives) showed a negative slope during the drift segment (hereafter referred to as 'negative' dives), while 602 dives showed a positive slope ('positive' dives). The mean maximum dive depth of drift dives across all seals (i.e. the deepest depth attained during a given dive) was 133.0±76.3 m and 115.0±80.3 m for negative and positive dives, respectively, and the maximum depth recorded for each individual varied from 85.2 m to 610.4 m. The drift segment generally occurred at depths between about 65 m and 117 m (Fig. 2) regardless of the direction of the drift. Negative drift segments started at 66.5±59.4 m and ended at 123.0±74.9 m (Fig. 2A), while positive segments started at 112.3±79.1 m and ended at 64.2±65.8 m (Fig. 2B).

The frequency distribution of drift rates showed a clear bimodal pattern, and very few dives had a drift rate around zero (Fig. 3). Negative drift rates were on average –19.9±8.2 cm s^{-1}, while positive rates were 16.0±11.9 cm s^{-1}. The 95% probability density range of observed drift rates was –33.4 cm s^{-1} to 23.1 cm s^{-1}.

Time series, fitted values and resolution

Time series with fitted spline curves are presented in Fig. 3. Although there were distinct individual variations, a clear general pattern of change in drift rate over time could also be seen. Trips could be broadly defined by three distinct phases similar to those obtained using daily travel rates (see e.g. Hindell et al., 1999; Le Boeuf et al., 2000; McConnell et al., 2002 and Results and Discussion below). The first phase lasted about 30–50 days, and most seals showed a gradual decrease in drift rate. Some seals initially had positive drift rates (i.e. they drifted upwards during the passive phase) but they all showed exclusively negative drift rates (i.e. sinking) by the end of this first phase. The second phase was characterised by an initial levelling out followed by a gradual increase in drift rate. Except for cases where the record stopped prematurely due to tag failure, loss or death of the animal, this second phase lasted roughly 100 days. Most of the

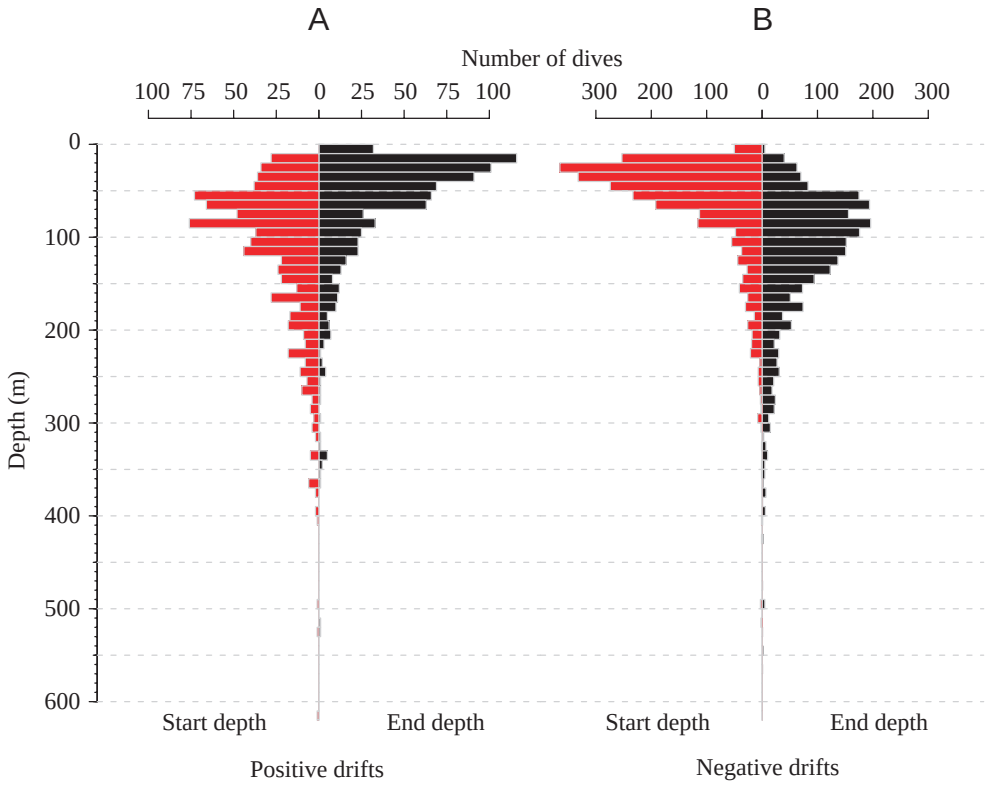

Fig. 2. Histograms showing the frequency distribution of start (red) and end (black) depths for the drift segments of (A) negative and (B) positive drift dives.

Table 1. *Details of the 24 Macquarie Island southern elephant seal pups for which drift dives were regularly observed in SRDL records*

		Dates			Mass (kg)			Duration[b] (days)		Positive daily change[c] (day after departure)			Phase duration[d] (days)			Days of change[e]	
Reference	Year	Weaning	Departure	Return	Weaning	Departure[a]	Return	Record	Trip	First	Max	Last	1	2	3	–	+
22483_96	1996	19 Oct	05 Dec		92			55		32	38	(48)	31	(16)		(14)	(12)
26623_96	1996	19 Oct	17 Dec		169			146		47	54	(128)	46	(81)		(35)	(8)
26624_96	1996	20 Oct	10 Dec		92			136		40	127	(136)	39	(96)		(31)	(34)
28482_96	1996	21 Oct	20 Dec		171			42		33	42	(42)	32	(9)		(8)	(0)
28504_99	1999	18 Oct	29 Dec	23 Jun	195	123	176	175	177	41	98	159	40	118	18	19	21
2846_99	1999	21 Oct	20 Dec	30 Jun	161	108	165	183	193	79	183	183	78	104	10	4	15
22488_99	1999	22 Oct	08 Dec	10 Jun	94	68		182	185	48	90	130	47	82	55	14	42
28497_99	1999	24 Oct	09 Dec	22 Apr	101	71	119	115	135	39	69	115	38	76	20	7	33
26627_99	1999	25 Oct	13 Dec	10 Jun	90	62	90	176	180	41	117	169	40	128	11	19	33
2849_99	1999	26 Oct	28 Dec	07 Jul	164	103	153	144	192	8	78	144	7	136	48	13	19
28494_99	1999	26 Oct	23 Dec	17 Jun	145	93	136	94	177				(94)			(14)	(1)
28496_99	1999	26 Oct	24 Dec		169	108		93		31	56	(66)	30	(35)		(46)	(18)
20918_99	1999	27 Oct	09 Dec	11 May	85	58	95	119	154	28	35	119	27	91	35	9	13
17217_99	1999	28 Oct	31 Dec	26 Jun	162	101	170	144	178	44	104	144	43	100	34	21	29
26629_99	1999	03 Nov	22 Dec		108	80		107		43	76	(107)	42	(64)		(29)	(41)
5812_99	1999	12 Nov	23 Dec	10 Jun	93	70		167	170	39	94	133	38	94	37	27	33
Cleo_00	2000	20 Oct	31 Dec		197	131		225		30	147	198	29	168		28	58
FirstOne_00	2000	26 Oct	25 Nov	30 Apr	78	59		57	156	7	16	44	6	37	112	16	28
Alice_00	2000	30 Oct	29 Dec	22 Jul	161	106		204	205	50	78	172	49	122	33	30	25
Ella_00	2000	01 Nov	31 Dec		175	114		98		44	93	(98)	43	(54)		(29)	(38)
Flora_00	2000	01 Nov	01 Jan		173	119		176		45	154	163	44	118		23	15
Billie_00	2000	06 Nov	28 Dec	17 Jul	180	113		198	201	58	111	176	57	118	25	54	34
Doris_00	2000	09 Nov	30 Dec	11 Aug	144	95		220	224	37	165	178	36	141	46	35	45
20918_00	2000	13 Nov	27 Dec	23 May	99	68		140	147	34	41	140	33	106	7	19	29
Mean		27 Oct	20 Dec	15 Jun	137.4	92.5	138	141.5	178.3	39	89.8	147.9	38	108.7	35.1	23	26
Min.		18 Oct	25 Nov	22 Apr	78	58	90	42	135	7	16	44	6	37	7	4	0
Max.		13 Nov	01 Jan	11 Aug	197	131	176	225	224	79	183	198	78	168	112	54	58
S.D.		7.6	10.2	30.9	40.2	23.4	33.7	51.6	23.6	14.6	44.6	36.7	14.6	30.2	26.6	12.31	14.26

[a]The departure mass is given as the last recorded mass, typically measured 4.2±3.3 days (mean ± S.D.) prior to the last sighting of the individual at the Isthmus study colony. The departure mass on the actual day of departure was estimated by extrapolation from the last recorded mass at a mean individual daily mass loss rate (the difference between weaning mass and last recorded mass divided by the number of days between them). Since the difference between the last recorded and estimated mass was typically very small (1.8±0.4 kg, or 1.97±0.3%), we have consistently used the last recorded mass. [b]The record duration is the last day after departure at which data were received from a tag, while the trip duration is the number of days between departure and the first sighting of a seal back at Macquarie Island. [c]The first and last days for which a positive change in drift rate was observed are presented as day after departure ('First' and 'Last'), while 'Max' represents the day after departure at which the maximum positive change was observed. [d]The number of days between the first and last days for which a positive change in drift rate was observed. [e]The total number of days for which a negative (–) and positive (+) change in drift rate was observed.

Parentheses indicate that the number may not be accurate because of premature interruption of the record due to tag failure or death of the animal. These numbers were excluded from the calculations of the summary statistics presented at the bottom of the table.

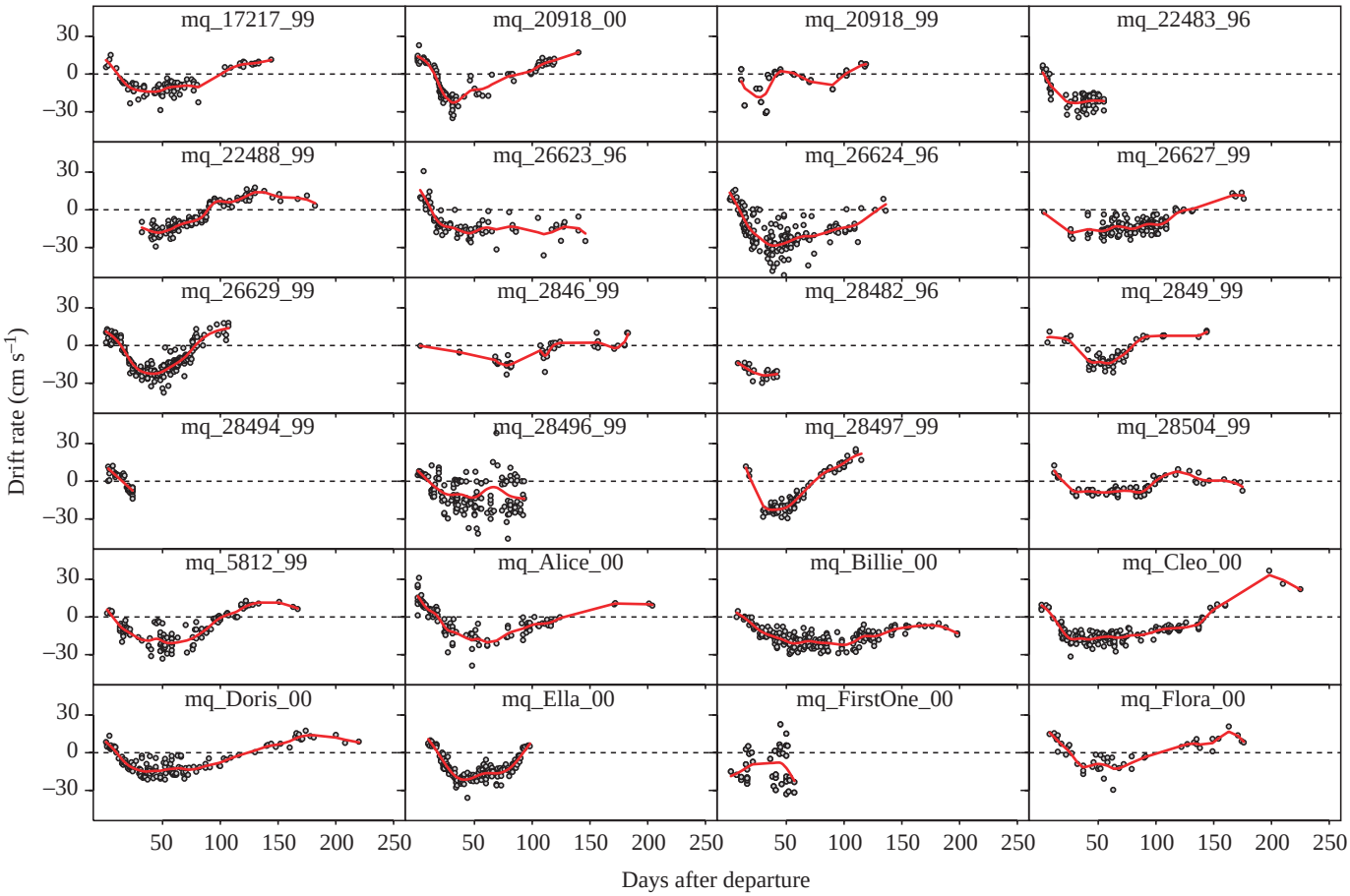

Fig. 3. Time traces of drift rates for each individual seal over the course of the first trip to sea. Each point represents a drift dive, while the solid red lines represent smoothed spline functions fitted by the GCV algorithm, constrained to an initial interval between spline knots of 14 days (see text).

seals showed positive drift rates at the end of this phase. In cases where the record lasted longer than the duration of phase 1 and 2, the drift rate either remained constant or decreased slightly throughout the third phase, until the end of the record.

There were large individual variations in drift rate changes over the course of the trip (Fig. 4). While some seals (e.g. 26629_99 and 28497_99) appeared to have a continuous period of negative change followed by a continuous period of positive change, others (most notably Billie_00 and Cleo_00) switched repeatedly between positive and negative change. The transitions between phases based on daily change in drift rate corresponded reasonably well with previous criteria using daily travel rate. For instance, the switch from negative to positive change in drift rate after the initial 'transit' period was generally associated with a sudden decrease in travel rate (Fig. 4). In general, the 90th quantile regressions of daily change in drift rate against daily travel rate indicated an upper 'edge' in the change in drift rate for any given daily travel rate. Although there were large individual variations, seals generally showed positive changes in drift rate only during days when their travel rate was less than ~50–90 km day^{-1} (median = 75.1 km day^{-1}; S.D. = 31.3 km day^{-1}), while negative changes in drift rate occurred at all travel rates (Fig. 5).

Temporal resolution of time series

The range of residuals of all drift rates for a given day over the fitted value for that day from the spline function varied between individuals from about –0.59 cm s^{-1} to 0.39 cm s^{-1}. The theoretical estimate of the total change in drift rate over the course of the assumed 100-day feeding period was 20 cm s^{-1}, corresponding to a daily change of 0.2 cm s^{-1}. The residual corresponding to the maximum kernel probability density was 1.31±0.43 cm s^{-1} (all seals combined). When we divided the residual values for each individual seal by the estimated mean daily change (e.g. 1.31/0.2), we obtained time intervals of 6.45±2.10 days (median = 6 days), over which any changes in drift rate are likely to reflect a biological trend as opposed to random variation.

Theoretical model of drift rate and body composition

Our mechanistic model of the predicted drift rates of an average-sized seal across the range of lipid contents is illustrated in Fig. 6. The three curves illustrate the variation in the relationship between lipid content and drift rates using various C_D values, while the vertical histogram represents the frequency distribution of all observed drift rates. The relationship between body composition and predicted drift rate

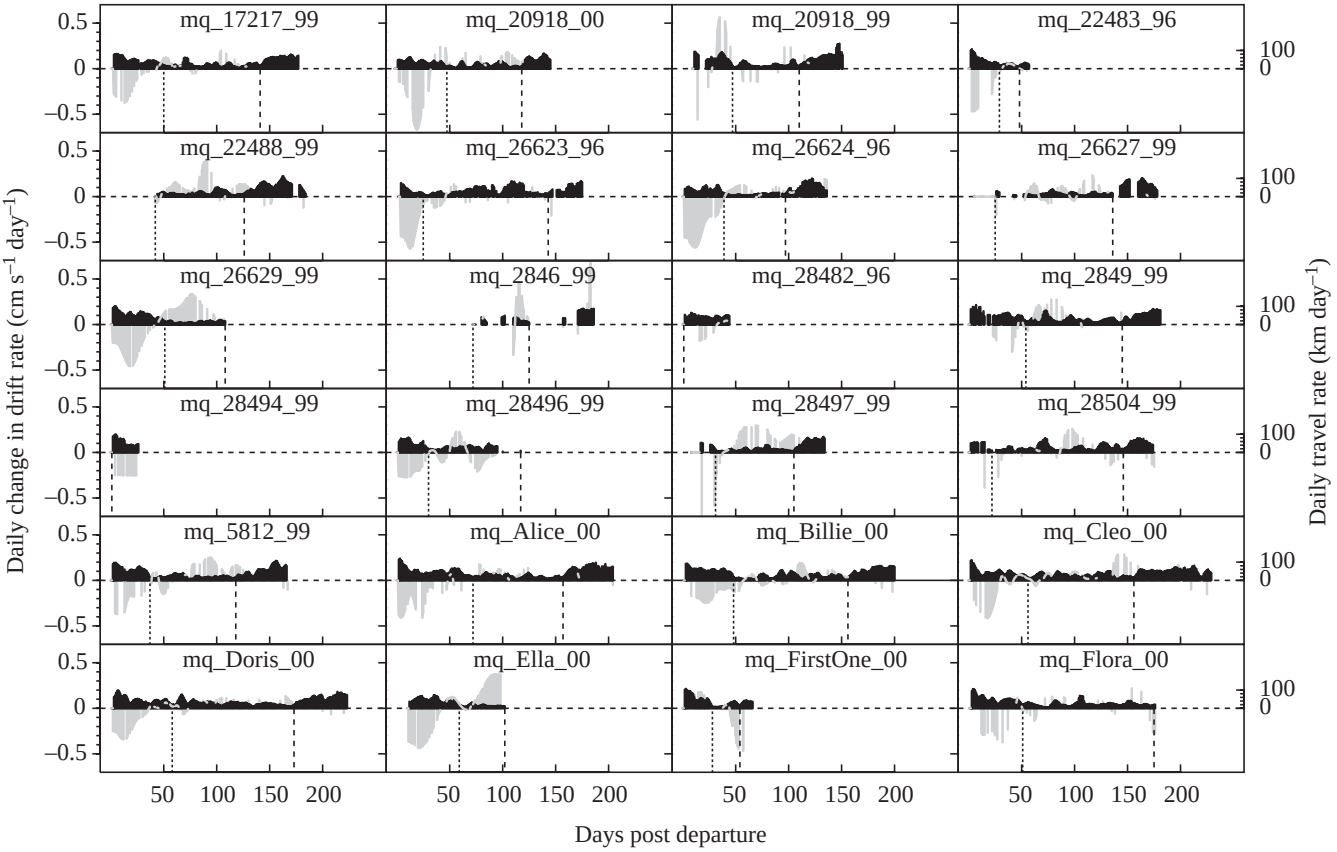

Fig. 4. Daily change in drift rate (grey bars) and daily travel rate (daily horizontal displacement; black bars) for individual seals over the course of the first trip. The vertical dotted and dashed lines indicate the switch between phase 1 and 2, respectively, based on the first and last day with a five-day running average of daily travel rate below 20 km (McConnell et al., 2002).

shows a clear sigmoid relationship with a high rate of change in drift rate for seals close to neutral buoyancy. This shape is a result of the quadratic relationship between velocity and drag (see equation 8). Using the C_D of a cylinder (1.17), the predicted drift rates ranged from –34.2 cm s^{-1} for a seal with 10% lipid to 27.5 cm s^{-1} for a seal with 60% lipid. The corresponding values using the C_D of a sphere (0.47) are –52.9 cm s^{-1} and 42.5 cm s^{-1}, respectively, while the C_D of a harbour seal swimming headfirst (0.09) results in extreme values of –123.5 cm s^{-1} and 99.2 cm s^{-1}, respectively.

1. Bias due to residual air in the lungs

Our model suggests that the buoyant force caused by residual air in the lungs can result in a significant positive bias in drift rate (Fig. 7A). At shallow dive depths, this extra buoyant force can be of similar magnitude to that caused by body lipid. For instance, at a depth of 10 m, the positive buoyant force attributed to lipid ranges from ~22 N to 120 N over the range of lipid contents while the corresponding value for residual air is ~28–14 N over the

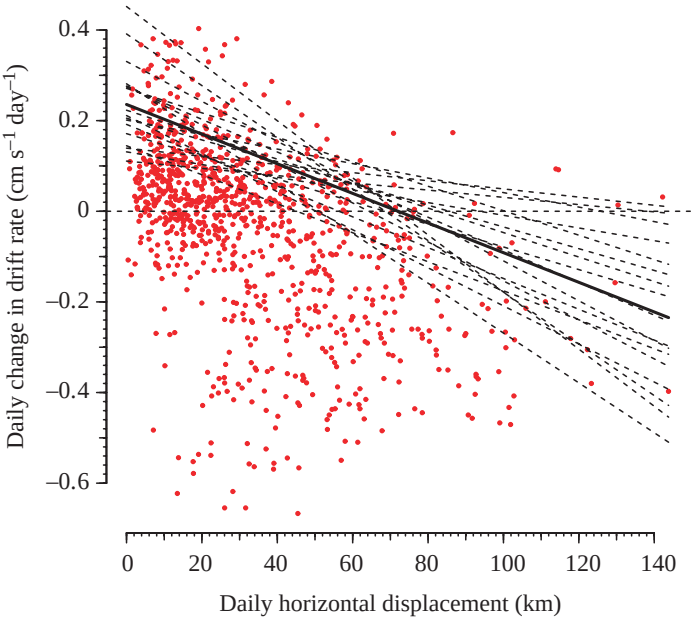

Fig. 5. Daily change in drift rate plotted against daily horizontal displacement (i.e. the distance between average daily locations). Each red point represents a drift dive. The thin dashed lines represent the 90th quantile regressions fitted for each individual seal, while the thick solid line represents the line obtained using the mean of the slopes and intercepts from each individual 90th quantile regression.

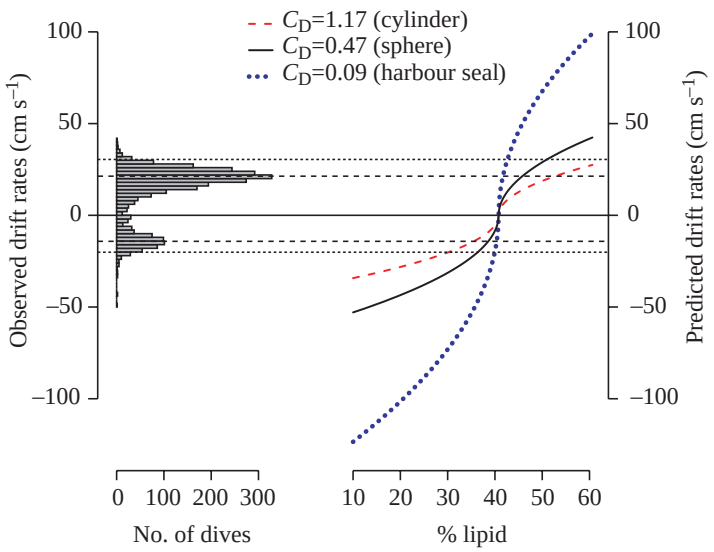

Fig. 6. Vertical frequency distribution of observed drift rates (left), and curves representing the predicted drift rates (assuming no residual air) of a seal with a total body volume of 100 litres (right). The three curves correspond to the predicted drift rates using published drag coefficients (C_D) for a cylinder (red dashed line) and a sphere (solid black line) from Vogel, 1981, as well as for a harbour seal (blue dotted line) from Williams and Kooyman, 1985. The horizontal dashed lines represent the maximum kernel density for all observed positive and negative drift rates separately, while the dotted lines represent the range of the 95% probability of occurrence (kernel density function, bandwidth = 2 cm s^{-1}).

same range. This means that at 10 m, residual air can provide more than half the total positive buoyant force for a lean seal (~64% at 10% lipid), while for a fat seal (60% lipid) residual air provides just over 10% of the buoyant force. This bias is substantially reduced at greater depths because of the exponential decrease in volume with increasing depth. For instance, at 50 m, residual air provides ~32% of the buoyant force for a seal with 10% lipid, while for a seal with 60% lipid, air provides less than 4% of the buoyant force. At 100 m, these figures are further reduced (~20% at 10% lipid and ~2% at 60% lipid).

Fig. 7B shows the relationship between lipid content and the expected drift rate for the model seal at the same depths as in Fig. 7A.

2. Error due to variations in body surface area and volume

Fig. 7C illustrates the relationship between lipid content and theoretical drift rate, allowing for variations in body surface area from 0.5 m^3 to 1.5 m^3. These errors are more pronounced towards the extremes of lipid contents and drift rates, while they approach zero for seals near neutral buoyancy.

3. Error due to variations in seawater density

The range of seawater temperature and salinities likely to be encountered by an elephant seal from Macquarie Island corresponds to a seawater density range of 1.027–1.030 g cm^{-3}. This represents about 2.5% of the range of densities for seals over the range of lipid contents (0.982–1.100 g cm^{-3}) and would result in a maximum error in predicted lipid content of 1.3% (Fig. 7D).

Model evaluation

1. Simulation test

Our sensitivity analysis indicated that the prediction accuracy was highly dependent on which parameters were kept constant and which were randomly selected from the pre-defined probability distributions. When all parameter values were randomly selected, 95% of the residuals of predicted *vs* actual lipid contents were between –7.3% and 6.4% lipid (Table 2). When seawater density was kept constant at 1.028 g cm^{-3} while allowing all other parameters to vary, this error range was reduced by only about 0.5%. The error reduction was slightly larger when we kept body surface area and volume constant while allowing all other parameters to vary (error reduction ~5.8%). The most dramatic reduction in prediction errors was achieved when the C_D was kept constant at 0.83, resulting in errors ranging from approximately –2.6% to 1.8% lipid. Our results indicate that while uncertainties in seawater density and body surface area and volume together are not likely to result in prediction errors of more than about ±2.5%, uncertainties in C_D can cause errors in lipid content of over 10%. Furthermore, the errors were highly dependent on the magnitude of positive or negative drift rate. The smallest errors were calculated for drift rates around zero while errors increased towards the extremes of the range of our data.

Table 2. *Results from the simulation analysis of the relative importance of errors in surface area and volume, seawater density and C_D on the prediction errors of lipid content from drift rates (see text and legend for Fig. 9 for further details)*

Parameter kept constant	Lower 95%	Mean	Upper 95%	Range	Error range reduction (%)
None	–7.30	–0.22	6.43	13.72	
Seawater density	–7.03	–0.01	6.62	13.65	0.52
Surface area and volume	–6.64	–0.21	6.29	12.93	5.79
Drag coefficient	–2.65	–0.20	1.80	4.45	67.54

Values in the first four columns represent percent lipid content, while values in the last column represent the percent reduction in the 95% error range relative to the error range when no parameters were kept constant [i.e. 100×(13.65/13.72)=0.52].

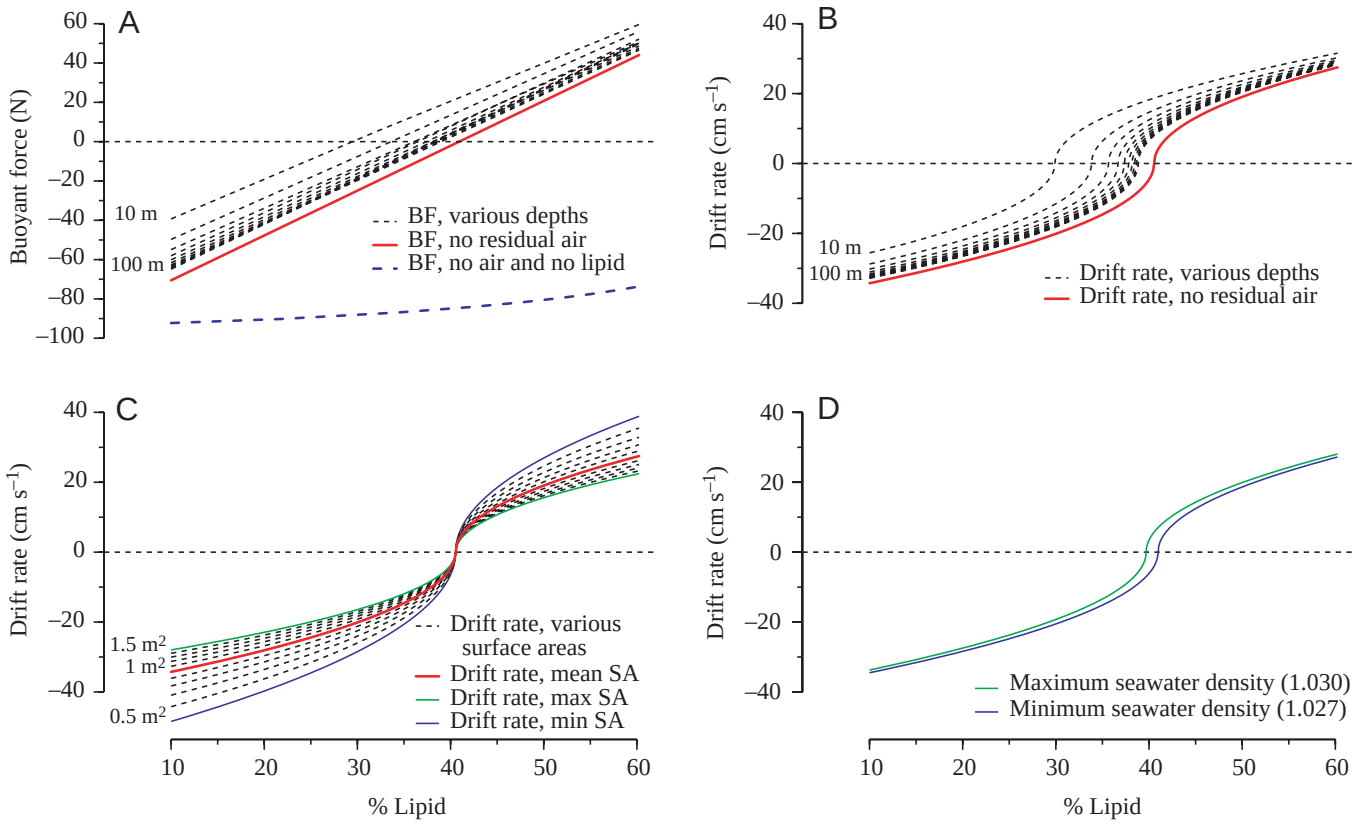

Fig. 7. Relationships based on theoretical calculations for a seal pup with a total volume of 100 litres. (A) Buoyant force attributed to different body components. The broken blue line represents the buoyant force (negative) of the total non-lipid body, while the red line represents the buoyant force of the whole body, including lipid but assuming no residual air. The broken black lines represent the buoyant force of the total body, including residual air left in the lungs at 10 m-depth intervals from 10 m to 50 m. (B) Drift rates predicted from equation 9 for the 100-litre seal, assuming a total surface area of 1 m^2. The red line represents the drift rate assuming no residual air in the lungs, while the broken black lines represent drift rate accounting for residual air at 10 m intervals from 10 m to 100 m. (C) Drift rate calculated from equation 9, assuming no residual air in the lungs. The red line represents drift rate assuming a surface area of 1 m^2 (i.e. identical to the red line in B), while the broken black lines represent the drift rate resulting from variations in surface area. The two extreme values of surface area, 0.5 m^2 and 1.5 m^2, are indicated by the blue and green lines, respectively. (D) Drift rates calculated from equation 9 using the minimum and maximum seawater densities (1.027 g cm^{-3} and 1.030 g cm^{-3}; blue and green curve, respectively) likely to be encountered by southern elephant seal pups from Macquarie Island. See text for further details.

2. Correlation between predicted and measured lipid content

Due to lack of body composition measurements and/or lack of drift dives early in the record, 12 seals were excluded from the following comparison. Table 3 presents data from the remaining 12 seals for which data were sufficient. There was a strong positive correlation between predicted and measured lipid contents using either of the two criteria used [see Methods; i.e. the 'minimum sum of squared residuals' (minimum SSR) criterion or the 'slope=1' criterion] for finding the optimal C_D value.

Minimum SSR criterion. The SSR was obtained using a C_D of 0.69 (SSR=19.03; Fig. 8). Using this C_D, the mean absolute difference between predicted and measured lipid contents was 1.39% (Table 3). The slope of the linear regression of measured against predicted drift rates was less than 1 [$\%TBL_m$=0.71($\%TBL_p$)+12.37; $F_{1,10}$=29.69, r^2=0.72], but the deviation from a slope of unity was not quite significant at the 0.05 level (*t*-test: t=–2.20, P=0.052). Lipid contents predicted from drift dives were underestimated for leaner seals compared with the measured lipid contents, while they were overestimated for fatter seals (Fig. 9).

Slope=1 criterion. We obtained a slope coefficient of 1 using a C_D of 0.49 ($\%TBL_m$=$\%TBL_p$+1.80; $F_{1,10}$=29.69, r^2=0.72; Fig. 8). This C_D resulted in predicted lipid contents that were on average 1.86% lower than those measured using labelled water (Table 3), and, because the slope was one, this bias was constant throughout the range of lipid contents (Fig. 9).

Using the C_D values obtained using the two criteria, we estimated the lipid content of each seal when this had reached its minimum value, i.e. at the transition between Phases 1 and 2 (Table 3). Using the minimum SSR criterion (C_D=0.69), the predicted lipid contents ranged from 23.3% to 32.7% (mean=27.6%), while the slope=1 criterion gave a higher mean (30.1%) but a smaller range (27.1–33.8%). However, the lowest predicted values generally occurred within

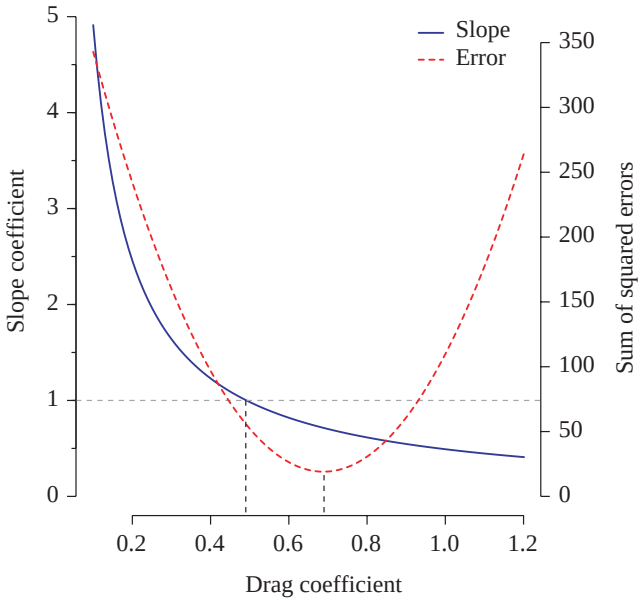

Fig. 8. Regression slope coefficient and sum of squared residuals between predicted and measured lipid contents expressed as functions of drag coefficients (C_D; ranging from 0.09 to 1.20) used in the predictive model of lipid content. The red line represents the sum of squared residuals (SSR) for each C_D value used, while the blue line represents the slope coefficient. The horizontal broken line represents a slope coefficient of 1, and the left-hand vertical broken line represents the corresponding C_D value (0.49). The right-hand vertical broken line represents the C_D value (0.69) that corresponded to the minimum SSR of predicted and measured lipid contents (see also Fig. 9).

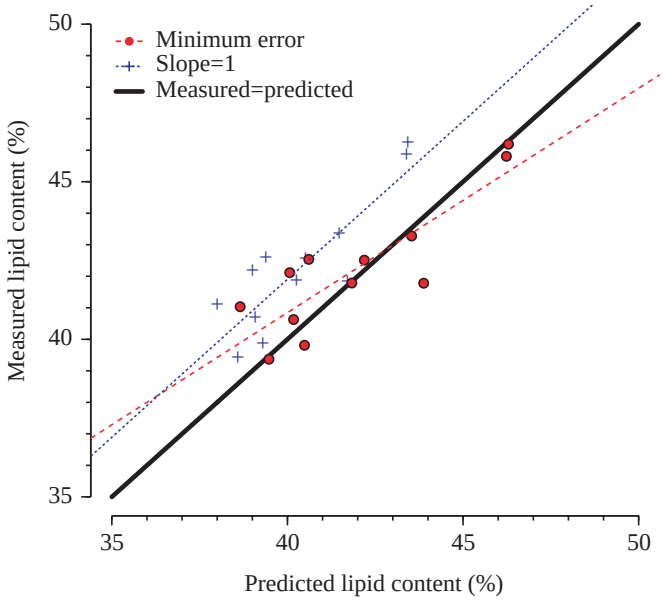

Fig. 9. Correlation between lipid content at the start of the trip, predicted from the fitted drift rates at departure (using the fitted spline function), for each individual seal and the lipid content measured just prior to departure using the labelled water method. The thick black line represents predicted lipid contents being identical to the measured lipid contents. The red circles (each circle representing an individual seal) were obtained using the drag coefficient (C_D) that minimised the sum of squared residuals between predicted and measured values (C_D=0.69), while the blue crosses (again, each cross representing one individual seal) represent the analysis using a C_D value that produced a regression slope of unity (C_D=0.49; see text and Fig. 8). The regression lines for these two models are represented by the red and blue broken lines, respectively (see text for regression results). Individuals for which the first daily fitted drift rate (and predicted lipid content) occurs more than 10 days after departure (20918_99, 28497_99 and 28504_99; see Table 3), and/or for which the initial fitted drift rate (and predicted lipid content) was calculated from one isolated drift dive early in the record followed by a long gap in the data (2846_99 and 26627_99) were excluded from the graph and the analysis. Also, one individual (FirstOne_00) for whom the drift dive record shows an unusual pattern, and is thus probably subject to significant dive misclassifications, has also been excluded.

~30–100 days after departure or ~80–150 days after weaning but varied substantially between individuals (Table 3).

Discussion

In this study, we have demonstrated how drift dives can be used to estimate the body composition of free-ranging elephant seals. This idea has been proposed before (e.g. Crocker et al., 1997; Webb et al., 1998), but our study expands these ideas and presents a quantitative analysis of the influence of various assumptions and potential sources of error and bias. The method makes use of simple dive characteristics, as recorded by readily available data logging and telemetry instruments, and therefore does not require the use of specialized sensors. If the recorded data are transmitted *via* satellite, the method also allows us to monitor the changes in body composition as they occur, even in animals that do not return to a place where they can be recaptured and measured. The cause of a particular change in relative body composition may not always be known (i.e. an increase in relative lipid content may occasionally be a result of selective protein depletion rather than lipid assimilation; see Discussion below), but this method may nevertheless provide important clues about the spatial and temporal distribution of foraging. Although drift dives have so far only been documented for elephant seals, other species may display dive characteristics that can be used in a similar way to estimate body condition.

General temporal changes in drift rate

The general division of the trips into three phases based on the first and last days of positive change in drift rate (Figs 3, 4) agreed well with the transition days based on the travel rate threshold used by, for example, Le Boeuf et al. (2000) and McConnell et al. (2002). Our data suggest that the initial 30–50-day period is characterised by relatively high travel rates and a gradual decrease in buoyancy, presumably as a result of depletion of onboard lipid stores. The switch from a decrease to an increase in buoyancy is not abrupt and is followed by a longer period (~100 days) of overall increase in

drift rate and buoyancy caused by increasing lipid stores. While some individuals show a gradual increase in drift rate and buoyancy, others appear to go through cycles of energy gain and energy loss (Fig. 4). These cycles of increase and decrease in drift rate are sometimes correlated with travel rate, possibly reflecting seals moving between profitable prey patches. At other times, seals appear to be in negative energy balance despite slow travel rates (Figs 4, 5), possibly reflecting foraging in less profitable patches. During the last phase, there was again a slight decrease in drift rate and buoyancy while seals were in transit back to the island.

The correspondence between travel rate and change in drift rate is not perfect, and there often appears to be a time lag between changes in travel rate and changes in drift rate. For instance, the ingestion of a prey item may not necessarily be followed by an immediate positive change in drift rate. Although lipid from prey may be assimilated into the blubber tissue relatively rapidly, the excretion of residual material as faeces may take longer. These residual materials are likely to be of similar or higher density to that of seawater and may result in a decreased overall buoyancy of the animal. However, captive studies on juvenile southern elephant seals indicate that the passage rate of faecal matter is in the order of 10–20 h (Krockenberger and Bryden, 1994), and the delay between prey assimilation and increased buoyancy caused by this factor is therefore unlikely to be significant over greater time scales.

The time lags between changing daily travel rates and daily change in drift rate may occasionally be the result of sampling errors. For instance, the daily travel rates have been calculated from ARGOS locations, which are subject to error (e.g. Vincent et al., 2002). However, we expect these errors to be relatively insignificant in relation to the distances covered by southern elephant seals, especially since we have used daily locations based on averaging over several location fixes.

Mechanistic model and sources of error

Drag, buoyancy and drift rate

The sigmoid shape of the relationship between lipid content and predicted drift rate has important implications for using drift rate to predict body composition. For animals close to neutral buoyancy, a small change in body composition (and thus buoyant force) will cause a large change in drift rate, while

Table 3. *Correlation between lipid contents at departure measured using the labelled water method and lipid contents at the start of the SRDL record predicted using the* C_D *of a sphere (0.49)*

	Departure lipid content (%)					Minimum lipid content[a] (%)			
		Minimum error (C_D=0.69)		Slope = 1 (C_D=0.49)		Min. error (C_D=0.69)	Slope = 1 (C_D=0.49)	Days after[b]	
Reference	Measured lipid content	Predicted lipid content	Residual[c]	Predicted lipid content	Residual[c]	Predicted lipid content	Predicted lipid content	Departure	Weaning
2846_99	43.29	36.28*	7.01*	36.45*	6.84*	29.06	31.18	77	137
28497_99	37.18	42.14*	–4.97*	53.31*	–16.13*	24.16	27.70	38	84
28496_99	42.12	40.07	2.05	38.99	3.13	30.15	31.95	93	152
26627_99	43.15	34.78*	8.37*	36.07*	7.08*	25.27	28.49	27	76
28494_99	42.51	41.37	1.15	40.5	2.01	32.69	33.76	24	82
17217_99	41.79	41.83	–0.04	40.24	1.55	29.25	31.31	42	106
2849_99	41.04	39.21	1.83	37.99	3.05	30.01	31.85	58	121
5812_99	40.63	39.53	1.10	39.07	1.56	25.07	28.34	57	98
Cleo_00	39.81	40.48	–0.67	39.29	0.52	28.41	30.72	42	114
FirstOne_00	23.1	25.56*	2.46*	28.53*	–5.43*	23.34	27.11	57	87
Ella_00	45.81	41.25*	4.56*	43.37*	2.44*	26.61	29.44	41	101
Alice_00	41.78	43.88	–2.10	41.7	0.08	27.01	29.72	63	123
Flora_00	46.19	43.53	2.66	43.41	2.78	30.62	32.28	65	126
Billie_00	39.37	37.9	1.47	38.57	0.8	26.24	29.18	100	152
Doris_00	42.54	40.61	1.93	39.38	3.16	28.99	31.12	36	87
20918_00	43.28	43.54	–0.26	41.46	1.82	24.75	28.12	32	76
Mean	40.85	41.09	1.39[†]	40.05	1.86	27.60	30.14	53.25	107.63
S.D.	5.24	1.95	0.82[†]	1.61	1.09	2.68	1.90	22.42	25.56
Min.	23.10	37.90	–2.10	37.99	0.08	23.34	27.11	24	76
Max.	46.19	43.88	2.66	43.41	3.16	32.69	33.76	100	152

*Excluded from summary statistics and correlation analysis (see below and text).

[†]Calculated from the absolute residual values.

[a]Minimum lipid content refers to the lowest predicted lipid content observed.

[b]Number of days after departure and weaning at which minimum drift rate occurred.

[c]The difference between the actual and predicted lipid content.

an equivalent change will result in a smaller change in drift rate for fatter and leaner seals. We may therefore expect smaller prediction errors in body composition around a drift rate of zero, while these errors should increase towards both extremes of drift rate and lipid content.

Surface area and volume

For animals like elephant seals that perform extended foraging trips lasting several months and that have a life history characterized by dramatic cycles of fasting and feeding, surface area and body volume are likely to change significantly over the course of the trip. This is particularly true in the case of juvenile animals that grow continuously during the time spent at sea. These changes will influence the drag resistance as well as the buoyancy and may lead to errors in our predictions of body composition from the observed drift rates. Because drag is directly proportional to the surface area, errors in our estimates of this area will have greater influence on our lipid content predictions towards the extremes of drift rate and lipid content, whereas these errors should approach zero when the buoyancy approaches neutral. However, based on all seals measured before and after this first foraging trip (Sea Mammal Research Unit, unpublished data), surface area for an average seal is estimated to change from ~0.8 m^3 at departure to ~1.1 m^3 at return. For a seal with an average body composition (~25–35% lipid), this would correspond to an error in predicted lipid content of no more than ~2%. This is further supported by our simulation analyses, which suggest that errors in estimated surface area and volume contribute only slightly to the overall prediction errors (Table 2).

Residual air

As illustrated in Fig. 7A,B, residual air in the lungs can have a significant influence on our predictions of body composition, and this bias will depend on the depth over which the drift segment occurs. Again, for an observed drift rate of –23 cm s^{-1}, we would predict a lipid content of ~27% if residual air is not accounted for, while the actual lipid content would be about 14%, 23% or 25% if the drift rate was measured at 10 m, 50 m or 100 m depth, respectively. This prediction bias can either be reduced, by excluding dives shallower than a specified depth (e.g. ~4% and 2% bias when excluding all dives of <50 m and <100 m, respectively), or the bias can be controlled for by estimating the residual lung volume for a given individual at a representative depth of each dive (e.g. a depth halfway between the start and end depths of the drift segment). We should also point out that seals in this study showed a greater variability in drift rate during shallow dives (<100 m) compared with deeper dives. This may be a result of seals voluntarily adjusting the volume of residual air to optimise buoyancy during shallow dives. This effect would obviously disappear at greater depths due to the exponential decrease in air volume by depth, reducing the variability in drift rate. Minamikawa et al. (2000) showed that loggerhead turtles (*Caretta caretta*) perform dives during which they remain at a particular depth without actively swimming and that they select the depth in order to maintain neutral buoyancy. Although this so-called 'residence depth' is affected by the amount of air in the lungs, turtles do not appear to actively determine this depth by adjusting the amount of air. However, Sato et al. (2002b) argue that king (*Aptenodytes patagonicus*) and adelie (*Pygoscelis adeliae*) penguins voluntarily regulate the air volume at the start of a dive depending on the expected duration of the dive in order to optimise the costs and benefits of buoyancy.

Seawater density

Although elephant seals perform long migrations and deep dives, crossing many sharp temperature and salinity gradients, the maximum range in seawater density encountered by seals in this study is very small in relation to the variations in body density, and our simulation tests showed that errors in seawater density account for only a small proportion (<1%) of the overall errors (Table 2; Fig. 7D).

Drag coefficient

Our simulation tests indicate that C_D was the most important factor contributing to the overall uncertainty in predicted lipid content (Table 2), even though the range of C_D values in this analysis was limited to values between 0.47 (sphere) and 1.17 (cylinder). Our previous analyses (see Fig. 6) suggest that C_D values of the magnitude observed for various streamlined objects (including fish and marine mammals) at similar Reynolds numbers [C_D ~10^{-4}–10^{-2} (Vogel, 1981)] are unrealistic, and we consequently excluded C_D values smaller than that of a sphere (0.47) from this analysis. Randomly selecting the C_D from values between that of a sphere and that of a cylinder accounted for over 90% of the total error attributed by surface area and volume, seawater density and C_D combined.

Predicted and actual lipid content

There was a strong correlation between lipid content predicted using drift rates and the lipid content estimated using labelled water (Fig. 9). When volume, surface area and residual air volume were estimated from morphometric measurements prior to departure, we were able to estimate lipid content at the start of the trip to within a few percent (Table 3). We were also able to obtain a good estimate of the most likely range of drag coefficients by allowing this to be fitted as a parameter by the model. Our results suggest that, while drifting passively through the water column, the C_D of our seals was in the range of ~0.49 (using the slope=1 criterion) to 0.69 (using the minimum SSR criterion). At Reynolds numbers between 10^4 and 10^6, the C_D of a sphere is ~0.47 (see above), while a prolate spheroid travelling crosswise has a C_D of ~0.59. It is important to emphasize that we should not expect C_D to be constant. The drag force acting on animals is likely to vary as a result of postural changes in response to perceived conditions, and this could have a confounding effect on the interpretation of buoyancy data. However, if drift dives are indeed resting dives, as was proposed by Crocker et al. (1997), it would make sense

for a seal to minimise its vertical movement while remaining passive. This could be accomplished by using the flippers as brakes or trim tabs. Such behavioural adjustments would further increase the drag force and may explain the discrepancy between the C_D value for a prolate spheroid (~0.59) and our upper estimate (0.69).

Although our analyses have provided a good estimate of C_D for a phocid drifting passively in a direction different from that of normal travel (headfirst), further experiments in the laboratory and in the field may improve our understanding of this behaviour. For instance, the C_D of a seal or seal-like body moving at different angles relative to the surrounding fluid could be measured in the lab, where these angles, as well as the speed, can be controlled. Another promising development is that of accelerometer loggers that can be attached to animals to measure swimming activity and body orientation. These instruments have already been used to identify fine-scale movements such as so-called 'burst-and-glide' swimming in free ranging cetaceans, seals and penguins (e.g. Nowacek et al., 2001; Sato et al., 2002b). Sato et al. (2003) have also measured the swimming activity and body orientation of free-ranging Weddell seals (*Leptonychotes weddellii*) and found that, while fatter seals predominantly showed burst-and-glide swimming on descent, leaner seals were able to glide throughout most of this descent phase. These findings suggest that it may be possible to monitor changes in body composition of seals that do not regularly perform drift dives. Other indices may be used such as the depth at which seals stop flipper beating on descent, the ratio of burst-to-glide periods or the rate of deceleration of a seal after each burst.

Although such experiments would improve the technique, our simple model still allowed us to make some inferences about changes in body composition of seals while at sea. At the start of their first trip, after the ~5–8 week post-weaning fast on land (Sea Mammal Research Unit, unpublished data), the fattest individuals had a measured lipid content almost twice that of the leanest seals (range: ~23–46%; Table 3). Our model estimated that seals reduced their relative lipid content by between ~7% and ~20% during the first ~50 days of the trip and that the lipid content at the transition between phases 1 and 2 was ~23–33% (Table 3). McConnell et al. (2002) estimated the time to protein and fat starvation for southern elephant seal pups using measurements of mass loss and changes in body composition during the post-weaning fast on land (Arnbom et al., 1993; Carlini et al., 2001), assuming that the metabolic rate was similar at sea and on land. They estimated the mean time to protein and fat starvation, respectively, as 70.2 days and 77.9 days for small (light) seals and 81.1 days and 113.8 days for large (heavy) seals and suggested that, while light seals would have reached critical levels at the end of Phase 1 (defined using the travel rate criterion), heavy seals would still be in relatively good condition at this transition. These estimates are generally lower than the ~80–150 days between weaning and the occurrence of the minimum lipid content estimated from drift rates in this study (Table 3). However, the changes in drift rate indicate that the change from negative to positive energy balance was not abrupt. Instead, the rate of negative change started declining around 25–30 days after departure (roughly 60–100 days after weaning; Figs 4, 6; Table 1), and, even at the time of minimum drift rate (and lipid content), all our seals still appeared to have sufficient energy reserves [i.e. a lipid content of ~23–33% compared with the estimated critical level of 10% (Cahill et al., 1979; McConnell et al., 2002)]. This may indicate that most pups start feeding gradually while still in transit, thereby reducing their rates of energy depletion and avoiding reaching critical levels. It is also possible that seals have a suppressed metabolic rate while at sea compared with when resting on land (Hindell and Lea, 1998) and that the times to fat and protein starvation reported by McConnell et al. (2002) are slightly underestimated.

Conclusion

To our knowledge, this is the first time that changes in body composition of free-ranging phocids have been estimated at sea. We have demonstrated that a thorough analysis of drift rate is a valuable tool for monitoring the changes in body composition of free-ranging marine animals and can be used to predict body composition to within a few percent. Our model also allowed us to estimate the minimum body composition of seals at the end of the transit from the island to their foraging grounds. Our estimates suggest that the energy stores of these naïve seal pups are unlikely to approach critically low levels before the onset of feeding. We believe that this approach is a valuable extension to the current use of data recorders and telemetry and that it has the potential of providing more-accurate and finer resolution data on important feeding areas and seasons for large marine predators and may therefore be used as a basis for more informed management decisions for species exploiting distant areas of the oceans over long time periods.

We are very grateful to the members of the 1998–1999, 1999–2000 and 2000–2001 Australian National Antarctic Research Expeditions (ANARE) for their assistance in the field, especially to Kathryn Wheatley (who also provided invaluable assistance with isotope analyses), Iain Field, Rupert Davies, John van den Hoff, Clive McMahon, Tore Pedersen, Julian Harrington, Alice Parker, Matt Pauza, Megan Tierney and Andrew Welling. We wish to acknowledge the invaluable technical expertise of Phil Lovell and Colin Hunter during the many years of tag and telemetry system development. We also wish to thank Dave Thompson, Mark Hindell, Sascha Hooker and Christophe Guinet for stimulating discussions throughout the development of the manuscript, and two anonymous reviewers for extensive comments that greatly improved the quality of the paper. This work was supported by a NERC Small Grant (CR9/04605), and additional funding to the first author was provided by the Swedish Antarctic Research Program (SWEDARP) 1998–99, the Ymer-80 Foundation and the Percy Sladen Foundation. C.J.A.B. was supported by the Natural Sciences and Engineering Research Council of Canada (NSERC) and the

Australian Research Council (ARC). All animal procedures were carried out under Antarctic Animal Ethics Committee approval (ASAC permit 2265) and in accordance with UK Home Office License Regulations.

References

Argos (1989). *Guide to the Argos System*. Toulouse: Argos CLS.

Arnbom, T., Fedak, M. A., Boyd, I. L. and McConnell, B. J. (1993). Variation in weaning mass of pups in relation to maternal mass, postweaning fast duration, and weaned pup behavior in southern elephant seals (Mirounga-leonina) at South-Georgia. *Can. J. Zool.* **71**, 1772-1781.

Beck, C. A., Bowen, W. D. and Iverson, S. J. (2000). Seasonal changes in buoyancy and diving behaviour of adult grey seals. *J. Exp. Biol.* **203**, 2323-2330.

Bekkby, T. and Bjorge, A. (1998). Variation in stomach temperature as indicator of meal size in harbor seals, *Phoca vitulina*. *Mar. Mamm. Sci.* **14**, 627-637.

Bell, W. J. (1991). *Searching Behaviour – The Behavioural Ecology of Finding Resources*. London: Chapman and Hall.

Bost, C. A., Georges, J. Y., Guinet, C., Cherel, Y., Putz, K., Charrassin, J. B., Handrich, Y., Zorn, T., Lage, J. and LeMaho, Y. (1997). Foraging habitat and food intake of satellite-tracked king penguins during the austral summer at Crozet Archipelago. *Mar. Ecol. Prog. Ser.* **150**, 21-33.

Boyd, I., Arnbom, T. and Fedak, M. (1993). Water flux, body-composition, and metabolic-rate during molt in female southern elephant seals (Mirounga-leonina). *Physiol. Zool.* **66**, 43-60.

Boyd, I. L. and Arnbom, T. (1991). Diving behavior in relation to water temperature in the southern elephant seal – foraging implications. *Polar Biol.* **11**, 259-266.

Cahill, G. F., Marliss, E. B. and Aoki, T. T. (1979). Fat and nitrogen metabolism in fasting man. *Hormone Metab. Res.* **2**, 181-185.

Carlini, A. R., Márquez, M. E. I., Ramdohr, S., Bornemann, H., Panarello, H. O. and Daneri, G. A. (2001). Postweaning duration and body composition changes in southern elephant seal (Mirounga leonina) pups at King George Island. *Physiol. Biochem. Zool.* **74**, 531-540.

Chappell, M. A., Shoemaker, V. H., Janes, D. N., Maloney, S. K. and Bucher, T. L. (1993). Energetics of foraging in breeding adelie penguins. *Ecology* **74**, 2450-2461.

Charrassin, J. B., Kato, A., Handrich, Y., Sato, K., Naito, Y., Ancel, A., Bost, C. A., Gauthier-Clerc, M., Ropert-Coudert, Y. and le Maho, Y. (2001). Feeding behaviour of free-ranging penguins determined by oesophageal temperature. *Proc. R. Soc. Lond. Ser. B Biol. Sci.* **268**, 151-157.

Crocker, D. E., le Boeuf, B. J. and Costa, D. P. (1997). Drift diving in female northern elephant seals: implications for food processing. *Can. J. Zool.* **75**, 27-39.

Davis, R. W., Fuiman, L. A., Williams, T. M., Collier, S. O., Hagey, W. P., Kanatous, S. B., Kohin, S. and Horning, M. (1999). Hunting behaviour of a marine mammal beneath the Antarctic fast ice. *Science* **283**, 993-996.

Fancy, S. G., Pank, L. F., Douglas, D. C., Curby, C. H., Garner, G. W., Amstrup, S. C. and Regelin, W. L. (1988). *Satellite Telemetry: A New Tool for Wildlife Research and Management. U.S. Department of the Interior, U.S. Fish and Wildlife Service Resource Publication 172*. Washington: US Fish and Wildlife Service.

Fedak, M., Lovell, P., McConnell, B. and Hunter, C. (2002). Methods for overcoming the constraints of long range telemetry of biological information from animals: getting more useful data from small packages. *Integ. Comp. Biol.* **42**, 3-10.

Fedak, M. A. (1992). *Real-time telemetry techniques: observing the behaviour and physiology of seals at sea with VHF and acoustic telemetry. Report to Workshop on Marine Mammal Tracking at Arlie House.* Warrington, VA: Northeast Fisheries Science Center.

Fedak, M. A., Anderson, S. S. and Curry, M. G. (1983). Attachment of a radio tag to the fur of seals. *J. Zool.* **200**, 298-300.

Fedak, M. A., Lovell, P. and Grant, S. M. (2001). Two approaches to compressing and interpreting time-depth information as collected by timed-depth recorders and satellite linked data loggers. *Mar. Mamm. Sci.* **17**, 94-110.

Field, I. C., Bradshaw, C. J. A., McMahon, C. R., Harrington, J. and Burton, H. R. (2002). The effects of multiple anaesthesia in using tiletamine and zolasepam on Southern elephant seals (*Mirounga leonina*) at Macquarie Island. *Vet. Rec.* **151**, 235-240.

Gales, R. and Renouf, D. (1993). Detecting and measuring food and water-intake in captive seals using temperature telemetry. *J. Wild. Man.* **57**, 514-519.

Garthe, S., Gremillet, D. and Furness, R. W. (1999). At-sea-activity and foraging efficiency in chick-rearing northern gannets *Sula bassana*: a case study in Shetland. *Mar. Ecol. Prog. Ser.* **185**, 93-99.

Georges, J. Y., Bonadonna, F. and Guinet, C. (2000). Foraging habitat and diving activity of lactating Subantarctic fur seals in relation to sea-surface temperatures at Amsterdam Island. *Mar. Ecol. Prog. Ser.* **196**, 291-304.

Gordon, A. L. (1988). Spatial and temporal variability within the Southern Ocean. In *Antarctic Ocean and Resources Variability* (ed. D. Sahrhage), pp. 41-56. Berlin: Springer Verlag.

Gu, C. and Wahba, G. (1991). Minimizing GCV/GML scores with multiple smoothing parameters via the Newton method. *SIAM J. Sci. Statist. Comput.* **12**, 383-398.

Guinet, C., Dubroca, L., Lea, M. A., Goldsworthy, S., Cherel, Y., Duhamel, G., Bonadonna, F. and Donnay, J. P. (2001). Spatial distribution of foraging in female Antarctic fur seals Arctocephalus gazella in relation to oceanographic variables: a scale-dependent approach using geographic information systems. *Mar. Ecol. Prog. Ser.* **219**, 251-264.

Hedd, A., Gales, R. and Renouf, D. (1996). Can stomach temperature telemetry be used to quantify prey consumption by seals? A re-examination. *Polar Biol.* **16**, 261-270.

Hindell, M. A. and Lea, M. A. (1998). Heart rate, swimming speed, and estimated oxygen consumption of a free-ranging southern elephant seal. *Physiol. Zool.* **71**, 74-84.

Hindell, M. A., McConnell, B. J., Fedak, M. A., Slip, D. J., Burton, H. R., Reijnders, P. J. H. and McMahon, C. R. (1999). Environmental and physiological determinants of successful foraging by naive southern elephant seal pups during their first trip to sea. *Can. J. Zool.* **77**, 1807-1821.

Hooker, S. K., Boyd, I. L., Jessopp, M., Cox, O., Blackwell, J., Boveng, P. L. and Bengtson, J. L. (2002). Monitoring the prey-field of marine predators: Combining digital imaging with datalogging tags. *Mar. Mamm. Sci.* **18**, 680-697.

Ihaka, R. and Gentleman, R. (1996). R: a language for data analysis and graphics. *J. Comp. Graph. Stat.* **5**, 299-314.

Klimley, A. P., le Boeuf, B. J., Cantara, K. M., Richert, J. E., Davis, S. F., van Sommeran, S. and Kelly, J. T. (2001). The hunting strategy of white sharks (*Carcharodon carcharias*) near a seal colony. *Mar. Biol.* **138**, 617-636.

Koenker, R. W. and Bassett, G. W. (1978). Regression quantiles. *Econometrica* **46**, 33-50.

Kooyman, G. L. (1965). Techniques used in measuring diving capacities of Weddell seals. *Polar Rec.* **12**, 391-394.

Kooyman, G. L. (1989). *Diverse Divers: Physiology and Behaviour*. Berlin: Springer-Verlag.

Kooyman, G. L., Cherel, Y., Lemaho, Y., Croxall, J. P., Thorson, P. H. and Ridoux, V. (1992). Diving behavior and energetics during foraging cycles in king penguins. *Ecol. Monogr.* **62**, 143-163.

Krockenberger, M. B. and Bryden, M. M. (1994). Rate of passage of digesta through the alimentary-tract of southern elephant seals (Mirounga-Leonina) (Carnivora, Phocidae). *J. Zool.* **234**, 229-237.

Le Boeuf, B. J., Crocker, D. E., Costa, D. P., Blackwell, S. B., Webb, P. M. and Houser, D. S. (2000). Foraging ecology of northern elephant seals. *Ecol. Monogr.* **70**, 353-382.

Le Boeuf, B. J., Naito, Y., Asaga, T., Crocker, D. and Costa, D. P. (1992). Swim speed in a female northern elephant seal – metabolic and foraging implications. *Can. J. Zool.* **70**, 786-795.

Lesage, V., Hammill, M. O. and Kovacs, K. M. (1999). Functional classification of harbor seal (*Phoca vitulina*) dives using depth profiles, swimming velocity, and an index of foraging success. *Can. J. Zool.* **77**, 74-87.

Lovvorn, J. R. and Jones, D. R. (1991a). Body mass, volume, and buoyancy of some aquatic birds, and their relation to locomotor strategies. *Can. J. Zool.* **69**, 2888-2892.

Lovvorn, J. R. and Jones, D. R. (1991b). Effects of body size, body fat, and change in pressure with depth on buoyancy and costs of diving in ducks (*Aythya* spp.). *Can. J. Zool.* **69**, 2879-2887.

McConnell, B. J. (1986). Tracking grey seals using service ARGOS. *Mesogee* **46**, 93-94.

McConnell, B. J., Fedak, M. A., Burton, H. R., Englehard, G. H. and

Reijnders, P. (2002). Movements and foraging areas of naive, recently weaned southern elephant seal pups. *J. Anim. Ecol.* **71**, 65-78.

McMahon, C. R., Burton, H., McLean, S., Slip, D. and Bester, M. (2000a). Field immobilisation of southern elephant seals with intravenous tiletamine and zolazepam. *Vet. Rec.* **146**, 251-254.

McMahon, C. R., Burton, H. R. and Bester, M. N. (2000b). Weaning mass and the future survival of juvenile southern elephant seals, *Mirounga leonina*, at Macquarie Island. *Antarctic Sci.* **12**, 149-153.

Minamikawa, S., Naito, Y., Sato, K., Matsuzawa, Y., Bando, T. and Sakamoto, W. (2000). Maintenance of neutral buoyancy by depth selection in the loggerhead turtle *Caretta caretta*. *J. Exp. Biol.* **203**, 2967-2975.

Moore, F. D., Olsen, K. H., McMurray, J. D., Parker, H. V., Ball, M. R. and Boyden, C. M. (1963). *The Body Cell Mass and its Supporting Environment: Body Composition in Health and Disease*. Philadelphia: W. B. Saunders.

Nagy, K. A. and Costa, D. P. (1980). Water flux in animals: analysis of potential errors in the tritiated water method. *Am. J. Physiol.* **238**, R454-R465.

Nowacek, D. P., Johnson, M. P., Tyack, P. L., Shorter, K. A., McLellan, W. A. and Pabst, D. A. (2001). Buoyant balaenids: the ups and downs of buoyancy in right whales. *Proc. R. Soc. Lond. Ser. B Biol. Sci.* **268**, 1811-1816.

Putz, K. and Bost, C. A. (1994). Feeding-behavior of free-ranging king penguins (*Aptenodytes patagonicus*). *Ecology* **75**, 489-497.

Putz, K., Wilson, R. P., Charrassin, J. B., Raclot, T., Lage, J., le Maho, Y., Kierspel, M. A. M., Culik, B. M. and Adelung, D. (1998). Foraging strategy of king penguins (*Aptenodytes patagonicus*) during summer at the Crozet Islands. *Ecology* **79**, 1905-1921.

Reilly, J. J. and Fedak, M. A. (1990). Measurement of the body-composition of living gray seals by hydrogen isotope-dilution. *J. Appl. Physiol.* **69**, 885-891.

Sato, K., Mitani, Y., Cameron, M. F., Siniff, D. B., Watanabe, Y. and Naito, Y. (2002a). Deep foraging dives in relation to the energy depletion of Weddell seal (*Leptonychotes weddellii*) mothers during lactation. *Polar Biol.* **25**, 696-702.

Sato, K., Naito, Y., Kato, A., Niizuma, Y., Watanuki, Y., Charrassin, J. B., Bost, C. A., Handrich, Y. and le Maho, Y. (2002b). Buoyancy and maximal diving depth in penguins: do they control inhaling air volume? *J. Exp. Biol.* **205**, 1189-1197.

Sato, K., Mitani, Y., Cameron, M. F., Siniff, D. B. and Naito, Y. (2003). Factors affecting stroking patterns and body angle in diving Weddell seals under natural conditions. *J. Exp. Biol.* **206**, 1461-1470.

Schreer, J. F. and Testa, J. W. (1996). Classification of Weddell seal diving behavior. *Mar. Mamm. Sci.* **12**, 227-250.

Tanaka, H., Sato, K., Matsuzawa, Y., Sakamoto, W., Naito, Y. and Kuroyanagi, K. (1995). Analysis of possibility of feeding of loggerhead turtles during internesting periods based on stomach temperature-measurements. *Nippon Suisan Gakkaishi* **61**, 339-345.

Venables, W. N. and Ripley, B. D. (1994). *Modern Applied Statistics With S-Plus*. New York: Springer-Verlag.

Vincent, C., McConnell, B., Ridoux, V. and Fedak, M. (2002). Assessment of Argos location accuracy from satellite tags deployed on captive grey seals. *Mar. Mamm. Sci.* **18**, 156-166.

Vogel, S. (1981). *Live in Moving Fluids*. Boston: Willard Grant Press.

Webb, P. M., Crocker, D. E., Blackwell, S. B., Costa, D. P. and le Boeuf, B. J. (1998). Effects of buoyancy on the diving behavior of northern elephant seals. *J. Exp. Biol.* **201**, 2349-2358.

Weimerskirch, H. and Wilson, R. P. (1992). When do wandering albatrosses *Diomedea exulans* forage? *Mar. Ecol. Prog. Ser.* **86**, 297-300.

Williams, T. M. and Kooyman, G. L. (1985). Swimming performance and hydrodynamic characteristics of harbor seals *Phoca vitulina*. *Physiol. Zool.* **58**, 576-589.

Wilson, R., Peters, G., Regel, J., Gremillet, D., Putz, K., Kierspel, M., Weimerskirch, H. and Cooper, J. (1998). Short retention times of stomach temperature loggers in free-living seabirds: is there hope in the spring? *Mar. Biol.* **130**, 559-566.

Wilson, R. P. (1992). Environmental monitoring with seabirds – do we need additional technology. *S. Afr. J. Mar. Sci.* **12**, 919-926.

Wilson, R. P., Putz, K., Gremillet, D., Culik, B. M., Kierspel, M., Regel, J., Bost, C. A., Lage, J. and Cooper, J. (1995). Reliability of stomach temperature-changes in determining feeding characteristics of seabirds. *J. Exp. Biol.* **198**, 1115-1135.